Geochimica et Cosmochimica Acta 402 (2025) 359–371

Contents lists available at ScienceDirect

Geochimica et Cosmochimica Acta

journal homepage: www.elsevier.com/locate/gca

Hydrothermal mobilization and molecular transformations of dissolved organic matter from deep subsurface sediments

Melina Knoke [a], Thorsten Dittmar [a,b], Jana Günther [a], Philipp Böning [a], Andreas Teske [c], Michael Seidel [a,*]

[a] Institute for Chemistry and Biology of the Marine Environment (ICBM), School of Mathematics and Science, Carl von Ossietzky Universität Oldenburg, Ammerländer Heerstraße 114-118, 26129 Oldenburg, Germany
[b] Helmholtz Institute for Functional Marine Biodiversity at Carl von Ossietzky Universität Oldenburg (HIFMB), Oldenburg, Germany
[c] Department of Earth, Marine, and Environmental Sciences, University of North Carolina, Chapel Hill, NC, USA

ARTICLE INFO

Associate editor: Elizabeth Canuel

Keywords:
DOM
Hydrothermal sediments
Carbon cycle
DOS
IODP Expedition 385
Guaymas Basin Tectonics and Biosphere

ABSTRACT

Carbon mobilization in hydrothermal sediments and advective transport of dissolved organic matter (DOM) to the ocean affect deep-sea ecosystems. However, the link between hydrothermal processes and DOM reactivity in organic-rich subsurface sediments, and the impact of DOM release on the marine carbon cycle remain poorly understood. The Guaymas Basin (Gulf of California), with its organic-rich sediments, hydrothermal vent sites, and magmatic sill intrusions is an ideal candidate for studying the hydrothermal influences on DOM biogeochemistry. We analyzed sediment and porewater samples from IODP Expedition 385 from down to ~330 m below seafloor and used hot-water Soxhlet extractions as a first-order approximation for simulating hydrothermal DOM mobilization. We assessed the molecular composition of solid-phase extractable (SPE) DOM via ultrahigh-resolution mass spectrometry (FT-ICR-MS) and quantified dissolved organic sulfur, nitrogen, and phosphorus (DOS_{SPE}, DON_{SPE}, DOP_{SPE}). We identified several biogeochemical processes transforming DOM: active microbial transformations in the upper sediments were related to enhanced DOM oxygenation, and elevated DON_{SPE} and DOP_{SPE} concentrations. Highly aromatic, probably recalcitrant DOM, accumulated under anoxic conditions in intermediate depths. Here, DOS_{SPE} concentrations were highest, probably due to abiotic sulfide incorporation into DOM. Hydrothermal alteration near magmatic sills reduced DOM molecular diversity and caused a significant shift in the chemical composition of deep subsurface sediments influenced by high temperatures. Our data indicated that hydrothermal sediments release DOM, including DOS_{SPE}, DON_{SPE} and DOP_{SPE}, to the ocean. Hence, hydrothermal discharge may not only sustain local benthic ecosystems by providing bioavailable DOM but also likely influences the deep-sea carbon pool by introducing recalcitrant DOM.

1. Introduction

Dissolved organic matter (DOM) is a ubiquitous complex organic mixture in aquatic ecosystems (Dittmar et al., 2021). Hydrothermal alteration contributes bioavailable (Hansen et al., 2019), and recalcitrant DOM to the ocean (Yamashita et al., 2023). However, hydrothermal circulation can also remove recalcitrant marine DOM (Hawkes et al., 2016; Hawkes et al., 2015; Rossel et al., 2017). Compared to surface oceanic carbon sources and sinks, hydrothermal systems contribute locally but significantly to the deep-sea carbon pool. It is therefore crucial to understand the impact of hydrothermal DOM mobilization in oceanic sediments on the overall marine carbon cycle.

The Guaymas Basin is a hydrothermal system with extensive thermal gradients and organic-rich sediments that can be sampled with sufficient resolution (Teske et al., 2021b), enabling us to characterize the hydrothermal contribution to the marine DOM pool. It is a young marginal seafloor spreading system beneath highly productive waters. High export production results in the rapid formation of these organic-rich sediments (Calvert, 1966). The sediments act as thermal blankets for magma emplacing into the sedimented flanking regions (Lizarralde et al., 2007). Shallow sill intrusions hydrothermally transform sedimentary organic matter into hydrocarbons, mobilize buried carbon, and drive hydrothermal fluid convection (Mara et al., 2024; Teske et al., 2021b). Petroleum generation from recently deposited sediments

* Corresponding author.
E-mail address: m.seidel@uni-oldenburg.de (M. Seidel).

https://doi.org/10.1016/j.gca.2025.06.005
Received 15 March 2024; Accepted 6 June 2025
Available online 8 June 2025

converts fresh photosynthetic biomass into hydrocarbons. The young hydrocarbon radiocarbon age (~5000 years) in the hydrothermally active southern axial trough of Guaymas Basin (Simoneit and Kvenvolden, 1994) indicates relatively fast petroleum migration to the sediment surface. A part of these petroleum compounds serves as substrates for microbial communities (Edgcomb et al., 2022; Kawka and Simoneit, 1987; Simoneit and Lonsdale, 1982; Teske, 2024).

Sulfurization of porewater DOM as an important abiotic transformation process in sulfidic sediments (Abdulla et al., 2020; Ksionzek et al., 2016; Pohlabeln et al., 2017), potentially increasing the recalcitrance of DOM. DOM sulfurization is fueled by the production of sulfide by sulfate-reducers in anoxic sediments (Damsté et al., 1989). Dissolved organic sulfur (DOS) release from sulfidic sediments contributes up to 39 % to the marine DOS pool (Ibrahim and Tremblay, 2023; Phillips et al., 2022).

Recent work by Brünjes et al. (2025) highlighted the significant role of hydrothermal transformations in shaping the DOM composition in young, organic-rich Guaymas Basin sediments (<50 cm below the seafloor). While near surface hydrothermal activity in the Guaymas Basin releases reactive DOM, contributing to a dissolved organic carbon (DOC) flux of up to 5 mmol C m^{-2} yr^{-1} (Lin et al., 2017), the potential for DOM mobilization of deep subsurface sediments remains largely unexplored. However, understanding these deeper hydrothermal organic matter transformations is crucial to assess their impact on long-term carbon sequestration and the marine carbon cycle. The objective of this study was to elucidate DOM dynamics in hydrothermally altered subsurface sediments in Guaymas Basin down to ~330 m depth. We hypothesize that different processes influence the DOM composition, depending on sediment depth and degree of diagenesis: 1) microbial transformations in younger sediments result in oxygenated DOM, enriched in nitrogen and phosphorus; 2) DOM accumulates in intermediate depths, and abiotic sulfurization leads to the formation of recalcitrant DOS; 3) hydrothermal alterations at high temperatures shape the molecular composition of DOM in the deep subsurface resulting in high saturation, low oxygenation and low molecular masses. We further hypothesize that both recalcitrant and bioavailable DOM persist in the subsurface sediments but can be released into the ocean when hydrothermal sill intrusions cause advective fluid flow.

2. Material and methods

2.1. Study site and sampling

IODP Expedition 385 with JOIDES Resolution (September 15th to November 15th, 2019) obtained sediment and porewater samples. Organic-rich sediments and sill intrusions in the off-axis region and the axial graben of the northern Guaymas Basin spreading segment were drilled (Sites U1545 to U1552, Fig. 1) (Teske et al., 2021b). The study area and the drilling sites have been surveyed previously (Teske et al., 2021b), as summarized in the Supplementary material.

We analyzed porewater and sediment samples from Sites U1545, U1547, U1550, and U1551 (Teske et al., 2021c–f). From the multiple holes drilled at each site, Hole B was dedicated to extensive microbial and biogeochemical sampling, including samples for this study. Perfluorocarbon tracers were deployed downhole on all cores to monitor drilling fluid contamination. Different drill technologies were deployed:

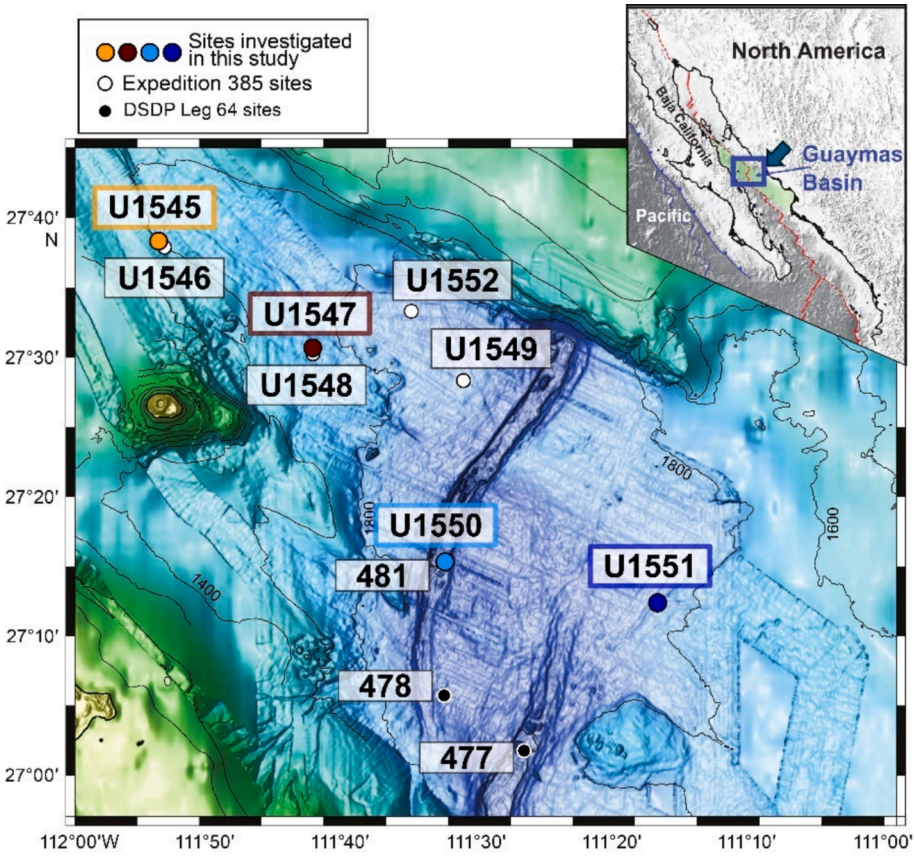

Fig. 1. Bathymetry of the Guaymas Basin (Gulf of California) showing the locations of all IODP Expedition 385 Sites (white and colored circles) and DSDP Leg 64 Sites (black circles) drilled in the region. This study specifically investigated Sites U1545, U1547, U1550, and U1551 (indicated by colored circles and colored text boxes). The inset map shows the location of the Guaymas Basin relative to North America, with the blue arrow indicating the zoom-in area and roughly marking the position of the Yaqui River estuary.
Adapted from Teske et al. (2021b).

an advanced piston corer (APC), a half-length APC (HLAPC), and an extended core barrel (XCB) system (Supplementary material). In-situ formation temperature measurements were taken with an APC temperature (APCT-3) and sediment temperature (SET2) tools (detailed description in Teske et al. (2021b)). Additionally, we analyzed seawater samples taken 2–3 m above the sediment near Site U1547 (Supplementary material).

Drilling at Site U1545 penetrated the sediment layers in the northwestern region of Guaymas Basin adjacent to a massive, thermally equilibrated sill between 350 and 430 m below seafloor (mbsf, Site U1546) (Teske et al., 2021b,c). Site U1547, situated at the hydrothermally active Ringvent area, targeted a shallow, recently emplaced hot sill, creating steep thermal gradients, driving hydrothermal circulation (Teske et al., 2019, 2021f). Here, the temperature increases rapidly towards the "Ring of Fire" where conspicuous hydrothermal activity and a topographical high of ca. 20 m mark the top rim of the buried sill (Teske et al., 2019). Site U1550 is situated near DSDP Site 481 (Curray et al., 1982), with heterogonous marine and terrestrial sediments accumulating in the northern axial valley (Teske et al., 2021d). Site U1551 represents the terrestrially influenced sediments of the southeastern Guaymas Basin, receiving riverine sand input from the Yaqui River (Teske et al., 2021e). In-situ temperature gradients categorize the drilling sites: The hydrothermally influenced Ringvent sediments with steep temperature gradients of 500–1000 °C km^{-1} (Site U1547), elevated temperature gradients of 200 to 250 °C km^{-1} at Site U1545, and the cooler Sites U1550 and U1551 with gradients of >100 °C km^{-1}. Even the coolest sites have temperature gradients twice as steep as commonly found for ocean crust (50–75 °C km^{-1}) (Kolawole and Evenick, 2023).

For context, we summarize previously published total organic carbon (TOC), sulfate (SO_4^{2-}), sulfide (H_2S), and ammonium (NH_4^+) (Supplementary material Fig. S1) as well as methane profiles (Supplementary material Fig. S2) (Teske et al., 2021c–f). TOC levels ranged between 2.56 and 4.87 %wt in the surface sediment and decreased downcore (Supplementary material Fig. S1a). Sulfate concentrations were highest in surface sediment interstitial water (between 24 and 28 mM at all sites) and decreased downcore (Supplementary material Fig. S1b). Sulfate-methane transition zones (SMTZ), identified by the simultaneous depletion of sulfate and methane concentrations, were located at 50 mbsf at U1545B, 110 mbsf at U1547B, 10 mbsf at U1550B, and 25 mbsf at U1551B (Supplementary material Fig. S2) (Bojanova et al., 2023; Teske et al., 2021c–e). Sulfide concentrations increased towards the SMTZs, reaching maximum values of ~8.9 mM (34–63 mbsf, U1545B), ~8.7 mM (113 mbsf, U1547B), ~8.5 mM (16 mbsf, U1550B), and ~115 μM (8 mbsf, U1551B), and then decreased with increasing depth (Supplementary material Fig. S1c). Ammonium concentrations were between 0.1 and 1.5 mM in near-surface sediments (<10 mbsf) and increased with increasing depth to maximum values of 30 mM (U1545B), 9 mM (U1547B), ~16 mM (U1550B), and 8 mM (U1551B) (Supplementary material Fig. S1d).

Sample handling on board is described in Teske et al. (2021a). In short, each sediment core was cut into 1.5 m sections and split for several analyses: whole-round core samples for on-shore analysis were either directly frozen at −80 °C or were pressed onboard for interstitial water analysis as described by Teske et al. (2021a). Seawater sampling is described in the Supplementary material and in Teske et al. (2019).

2.2. Soxhlet extraction

Hot-water Soxhlet extractions were performed after Schmidt et al. (2014) and Lin et al. (2017) with 20 g of sediment in pre-combusted (400 °C for 4 h) glass fiber thimbles (Whatman 603G, 30 × 100 mm). The Soxhlet system ran 48 h with 200 mL ultrapure water in the dark (further details in Supplementary material). Soxhlet extracts contain the water-extractable DOM fraction (DOM_{WE}).

Our hot-water extractions are a first-order approach that assesses the potential for DOM mobilization from the particulate phase and identifies DOM composition trends during hydrothermal mobilization, as demonstrated previously (Lin et al., 2017). We specifically used the same approach to maximize comparability with these previous data. Additionally, aqueous Soxhlet extraction serves as a practical alternative to interstitial water analysis for deeply buried sediments when FT-ICR-MS analysis of porewater is not feasible due to limited sample availability (Schmidt et al., 2014). This method has also been successfully used for the extraction of low-molecular-weight organic acids as potential substrates for microbes from the terrestrial deep biosphere (Vieth et al., 2008). Our setup maintained anoxic conditions to reflect the reducing environment of Guaymas Basin sediments. The ultrapure water used for extraction had a pH of ~7.0, which falls within the lower range of pH 7.0–8.2 in the natural sediments of our samples (Teske et al., 2021c–f). While the ultrapure water lacked initial salinity, the wet sediments contained residual porewater, helping to increase the ionic strength during extraction, thus reducing potential artifacts due to the absence of salting-out effects. Despite these considerations it is important to keep in mind that our simplified approach does not fully replicate in situ hydrothermal conditions. Natural hydrothermal sediments in Guaymas Basin experience different pressure regimes and a wide range of fluid temperatures from ~4 °C to >300 °C, whereas our extractions occurred at the boiling point of water (~100 °C, at atmospheric pressure). Hydrothermal fluid advection and petrogenesis also occur over much longer timescales than our 48-hour extractions. For example, batch extractions over 30 days yielded up to four times higher hot-water extractable DOC (DOC_{WE}) values than Soxhlet extraction (Lin et al., 2017), suggesting that our method likely provides a conservative lower estimate of the hydrothermally mobilizable DOM.

2.3. Elemental and molecular analysis

We filtered the porewater and water-extractable DOM_{WE} samples through glass fiber filters (GF/F Whatman, 0.7 μm, combusted at 400 °C for 4 h) and acidified them to pH 2 (HCl, p.a.).

DOC and total dissolved nitrogen (TDN) concentrations were determined by high-temperature catalytic oxidation with a Shimadzu TOC-V_{CPH} equipped with a TDN analyzer. Trueness and precision of DOC and TDN measurements were determined using deep-sea reference material (University of Miami, USA) and were better than 5 %. The DOC concentrations in the porewater (DOC_{PW}) are expressed in mM. The DOC_{WE} concentrations were normalized to TOC (Teske et al., 2021c–f) and expressed in percent of the initial TOC content (%TOC_{init}) as described in Lin et al. (2017). Values of DOC_{WE} %TOC_{init} represent the fraction of sedimentary organic carbon that can be hydrothermally mobilized as DOC. Higher values indicate a greater mobilization potential (e.g., from less altered sediments) compared to lower values indicating reduced mobilization potential (e.g., from more degraded or thermally altered sediments).

Porewater and water-extractable DOM were isolated via solid phase extraction (SPE) using PPL cartridges (Agilent Bond Elut PPL, 1 g) and methanol (HPLC grade, 99.8 %) as eluent as described in Dittmar et al. (2008). Acidified porewater and water-extractable DOM (pH 2) were adjusted with ultrapure water (pH 2) to a volume of 250 mL to increase the volume for SPE, using a maximum of 1 mg C per 1 g of PPL to avoid overloading the PPL cartridges (Supplementary material Table S1). For four porewater samples from Site U1551 only small volumes (<10 mL) were available, thus we combined those to two samples (Supplementary material Table S1). The extraction efficiency of SPE-DOM was 55.3 % ± 18.1 % (n = 134) (Supplementary material Table S1). We analyzed dissolved organic nitrogen of SPE-DOM (DON_{SPE}) concentrations by evaporating an aliquot of methanol extract, redissolving it in ultrapure water, and analyzing TDN with the Shimadzu TOC-V_{CPH} as described above.

We pipetted methanol extracts in pre-combusted 4 mL glass vials and redissolved them in 1 % HNO_3 to determine dissolved organic sulfur (DOS) and dissolved organic phosphorus (DOP) concentrations of SPE-

DOM (DOS_{SPE}, DOP_{SPE}) with an inductively-coupled plasma-optical emission spectrometer (ICP-OES, iCAP PRO, Thermo Scientific, Bremen, Germany) following Pohlabeln and Dittmar (2015) for DOS_{SPE}, extending the analytical window to include DOP_{SPE}. Instrumental drift and potential matrix effects were effectively compensated for by adding an internal standard prior to the ICP-OES measurements. Standard deviations of repeated measurements of the in-house SPE-DOM reference ($n = 10$, North Equatorial Pacific Intermediate Water) (Green et al., 2014) were below 6 % RSD (DOP_{SPE}) and 5 % RSD (DOS_{SPE}).

We analyzed the stable carbon isotopic composition of SPE-DOM on an elemental Analyzer (Flash 2000 EA) coupled via a Conflo IV interface to isotope ratio mass spectrometry (EA-IRMS, Thermo Scientific Delta V Plus) after pipetting methanol extracts into tin caps and completely drying it. Stable carbon isotope ratios are expressed as $\delta^{13}C$ relative to the Vienna Peedee Belemnite (VPDB) reference. For repeated analysis of a marine sediment reference, cross-referenced with certified international standard IAEA-CH-6, the trueness and precision were better than 0.2 and 0.1 ‰, respectively.

2.4. FT-ICR-MS analysis

We diluted an aliquot of SPE extract with ultrapure water and methanol (ULC/MS grade absolute) in a ratio of 1:1 (*v/v*) to a concentration of 1.8 mg DOC L^{-1} for molecular analysis with ultrahigh-resolution mass spectrometry. Samples were analyzed in duplicate using a 15 Tesla Fourier-transform ion-cyclotron-resonance mass spectrometer (FT-ICR-MS, SolariX XR, Bruker Daltonik, Bremen, Germany). We repeatedly measured North Equatorial Pacific Intermediate Water SPE-DOM as a reference to monitor instrument performance. Molecular formulae were attributed using the server-based tool ICBM-OCEAN (Merder et al., 2020). Analytical conditions and settings are given in the Supplementary material. Molecular formulae were grouped into operationally defined compound groups as described in Merder et al. (2020) according to their hydrogen-to-carbon (H/C) and oxygen-to-carbon (O/C) values and aromaticity index (AI_{mod}) (Koch and Dittmar, 2006, 2016). FT-ICR-MS signal intensities of masses with assigned molecular formulae were normalized to the sum of the intensities of all molecular formulae in each sample. We averaged replicate measurements, and considered only molecular formulae present in both duplicates.

To compare DOC_{PW} concentrations with the DOC_{WE} concentrations, we normalized DOC concentrations to the original TOC contents, expressed as DOC_{PW}* and DOC_{WE}* (Supplementary material Fig. S3):

1) **DOC_{WE}* (in g C kg^{-1} TOC^{-1}):** DOC_{WE} was normalized to the initial sediment TOC content and the amount of extracted sediment, accounting for the individual water volume used for each Soxhlet extraction (~200 mL).
2) **DOC_{PW}* (in g C kg^{-1} TOC^{-1})**: DOC_{PW} was normalized to the amount of sediment used for porewater extraction (sediment squeezing), the resulting porewater volume, and the specific TOC content of each sediment sample.

We then compared the DOM molecular compositions of porewater and Soxhlet extracts by scaling the average abundances of molecular compound groups to the DOC_{PW}* (or DOC_{WE}*) concentrations. This was done by multiplying the intensity-weighted relative abundance of each compound group by DOC_{PW}* (or DOC_{WE}*) concentration (in g C kg^{-1} TOC^{-1}) of each sample. The data were subsequently normalized across the entire dataset (i.e. for each compound group across all sites rather than within each individual site) to values between 0 (minimum) and 1 (maximum) as described previously (Seidel et al., 2017). This approach enabled us to compare the relative abundances of DOM compound groups between porewater and water-extractable DOM samples across all sites, considering different depths and sites with varying temperature gradients. Higher values indicate either a greater relative abundance in porewater (DOC_{PW*}) or a higher mobilization potential with hot water (DOC_{WE}*). This method was previously validated by Seidel et al. (2015) through a laboratory serial dilution of terrestrial and marine SPE-DOM samples from an Amazon River-to-ocean transect. These authors identified approximately 2,500 out of 3,600 molecular formulae with a significant ($p \leq 0.05$) linear response in the FT-ICR-MS, allowing for the calculation of their relative enrichment or depletion in natural samples.

Statistical analyses were performed with the R statistical platform (R Core Team, 2023). We used a principal coordinate analysis (PCoA) of the normalized molecular formulae intensities from FT-ICR-MS analysis. Centered and scaled environmental data and DOM molecular compound groups were fitted to PCoA ordination post hoc using the function *envfit* (permutations 10,000, $p < 0.05$) of the *vegan* package (Oksanen et al., 2022) in R (R Core Team, 2023). We calculated the degradation (I_{DEG}) (Flerus et al., 2012), the terrestrial (I_{Terr}) (Medeiros et al., 2016) and the porewater DOM sulfurization (I_{SuP}) (Knoke et al., 2024) indices from the molecular data to assess the influence of diagenesis and hydrothermal heating on the DOM composition (Table 1). Trends in DOM molecular diversity were assessed with help of functional diversity indices (D_F). The functional diversity index is based on Rao's quadratic entropy (Rao, 1982) as described in Mentges et al. (2017) and was calculated for the number of carbon atoms (D_F (C)), H/C values (D_F (H/C)) and the nominal oxidation state of carbon (NOSC) (LaRowe and Van Cappellen, 2011) (D_F (NOSC)) (Table 1). We correlated the relative intensity of molecular formulae with the sediment depth using Spearman's correlation ($\rho > 0.25$, $p < 0.024$). False-positive *p*-values were corrected after Benjamini and Hochberg (1995). The Wilcoxon–Mann–Whitney test was used to assess the significance of differences in SPE-DOM isotopic composition after normality was tested with the Shapiro-Wilk test, which indicated non-normal distributions.

Table 1
Overview and application of the calculated molecular DOM indices.

Index	Function	Reference
Degradation index (I_{DEG})	Indicates the degradation state of marine DOM. Higher values represent more degraded material (0–1).	Flerus et al. (2012)
Terrestrial index (I_{Terr})	Identifies terrestrial DOM from land-derived material. Higher values indicate higher abundance of terrestrial molecular formulae (0–1).	Medeiros et al. (2016)
Porewater sulfurization index (I_{SuP})	Indicates the abundance of sulfur-containing DOM from sulfidic sediments. Higher values indicate higher abundance of sulfurized molecular formulae (0–1).	Knoke et al. (2024)
Functional diversity index (D_F)	Quantifies the molecular diversity using Rao's quadratic entropy based on molecular properties listed below. Higher values indicate higher functional diversity and potentially younger DOM.	Mentges et al. (2017); Rao (1982)
D_F (C)	Represents diversity in the number of carbon atoms, indicating molecular size/mass, which are related to bioavailability.	Mentges et al. (2017)
D_F (H/C)	Indicates diversity in hydrogen-to-carbon (H/C) ratios, which reflect saturation, and bioavailability.	Mentges et al. (2017)
D_F (NOSC)	Represents diversity in the nominal oxidation state of carbon (NOSC), which is related to compound reactivity. Higher NOSC values indicate higher thermodynamic profit during microbial oxidation.	LaRowe and Van Cappellen (2011); Mentges et al. (2017)

3. Results

3.1. Porewater dissolved organic matter composition

DOC_{PW} concentrations increased with increasing sediment depth relative to the near-surface porewater samples (<10 mbsf, 0.44 mM to 1.3 mM) and to bottom seawater concentrations (Ringvent, ≤0.2 mM, Table 2) at all sites to maximum concentrations of 5.2 mM (>300 mbsf in U1545 and >125 mbsf in U1550, Fig. 2a–d). However, at Site U1547, DOC_{PW} concentrations were notably lower compared to the other drilling sites (DOC_{PW} < 0.8 mM, Fig. 2b).

TDN concentrations increased with sediment depth across all sites reaching 6 to 33 mM (Fig. 2e), being higher than bottom seawater (0.21 mM and 1.39 mM, Table 2) and near-surface porewater concentrations (0.12–3.14 mM, Table 2). DON_{SPE} increased in the upper 100 mbsf at all sites (up to 220 μM, Fig. 2f) compared to near-surface samples (13 to 47 μM, Table 2), with the smallest increase at Site U1547 (Fig. 2f). Yet, DON_{SPE} decreased in depths greater than 100 mbsf (Fig. 2f).

DOS_{SPE} and DOP_{SPE} concentrations followed trends of DON_{SPE} (Fig. 2g, h, Table 2): the concentrations were lowest in the near-surface samples and increased within the upper 100 mbsf (DOS_{SPE} 2.1 to ~200 μM, and DOP_{SPE} 0.11 to 1.9 μM, respectively). DOS_{SPE} and DOP_{SPE} concentrations decreased in sediment depths greater than 100 mbsf.

C/N_{SPE} values were between 9 and 13 in near-surface samples and 16 in the bottom seawater (Table 2) and reached values of >20 C/N_{SPE} in deeper samples (Fig. 2j). Similarly, C/S_{SPE} and C/P_{SPE} values increased with increasing sediment depth from ~11 to ~148 (C/S_{SPE}) and from 1128 to 10,538 (C/P_{SPE}) (Fig. 2k and l). Bottom seawater had values of 57 and 115 (C/S_{SPE}) as well as 1507 and 2902 (C/P_{SPE}) (Table 2).

Stable carbon isotope ratios ($\delta^{13}C$) of porewater SPE-DOM were, on average, −22.46 ± 0.27 ‰ (U1545), −23.12 ± 0.45 ‰ (U1547), −22.35 ± 0.43 ‰ (U1550), and −24.25 ‰ (U1551) (Supplementary material Fig. S4).

Intensity-weighted H/C values of SPE-DOM (from FT-ICR-MS analysis) increased with increasing depth (>1.3, >100 mbsf, Fig. 3a) compared to near-surface samples, bottom seawater and samples at Site U1551 (H/C < 1.4). In contrast, porewater SPE-DOM O/C values decreased with depth (0.35 to 0.42, near-surface sediment <10 mbsf, bottom seawater) to values below 0.36 (Fig. 3b).

Intensity-weighted average NOSC values generally decreased at depths >50 mbsf (Fig. 3c). Intensity-weighted average relative abundances of carboxyl-rich alicyclic molecules (CRAM) were >55 % in <50 mbsf in all cores and decreased to values ~50 % with increasing depth in all cores except for U1551 (Fig. 3d). The average DOM molecular mass (m/z) decreased with depth to values <325 Da compared to near surface porewater (<10 mbsf) and bottom seawater (335 to 400 Dalton, Da) (Figs. 3e and 4a).

Intensity-weighted relative abundances of molecular formulae containing N ranged between 39 (U1547, 3 mbsf) and 83 % (U1550, 28 mbsf) (Fig. 3f). Intensity-weighted relative abundances of DOM containing S ranged between 5 and 68 % and increased towards the respective SMTZ at all sites except U1551 (Fig. 3g), followed by downcore decreasing values. Intensity-weighted relative abundances of polycyclic aromatic (PCA) molecular formulae in porewater increased downcore to 5 % at 190 mbsf (U1545), ~3 % at 40 mbsf (U1547), ~2 % at 7 mbsf (1550) and 2 % at 23 mbsf (U1551) (Fig. 3h). The remaining DOM_{PW} groups and bottom seawater DOM composition are displayed in the Supplementary material Fig. S5 and Table S2.

I_{DEG} decreased with depth in all cores from 0.6 to <0.1 (Fig. 4c). I_{SuP} values were highest at the respective SMTZ of each core (>0.35), generally following the trends of profiles of DOS_{SPE} concentrations (Fig. 4d). I_{Terr} increased to downcore values >0.4 (Fig. 4e).

The functional diversity of H/C, this is D_F (H/C), increased downcore at Sites U1545 and U1547 to >0.15 at ~50 mbsf and then decreased to 0.12 (Fig. 4f). At Site U1550, D_F (H/C) reached values of approximately 0.12 except for values <0.12 at ~50 mbsf. The functional diversity of carbon numbers, D_F (C), and NOSC, D_F (NOSC), decreased downcore at Sites U1545, U1547 and U1550 to values <2.5 and 0.2, respectively (Fig. 4g and h). All D_F parameters increased with depth at Site U1551.

3.2. Carbon mobilization from sediments

Hydrothermally heated sediments from Sites U1545 and U1547 had lower potential to mobilize carbon (1–6 $\%TOC_{init}$) than Site U1550 at the axial trough and the terrestrially influenced Site U1551 (up to ~8 % TOC_{init}, Fig. 2i).

The $\delta^{13}C$ SPE-DOM values in the hot-water Soxhlet extracts (DOM_{WE}) were on average −21.88 ± 0.69 ‰ (U1545), −22.18 ± 0.06 ‰ (U1547), −22.14 ± 0.41 ‰ (U1550), −22.57 ± 0.40 ‰ (U1551). The values were relatively constant with depth in all cores (Supplementary material Fig. S4). A Wilcoxon rank sum test revealed a significant difference in $\delta^{13}C$ SPE-DOM values between DOM_{PW} and DOM_{WE} samples ($W = 288.5$, $p = 2.89 \times 10^{-5}$).

The molecular properties of DOM_{WE} differed between sites and with depth (Supplementary material Fig. S6). The average H/C values increased downcore (<1.24 to >1.24, Supplementary material Fig. S6a), whereas average O/C values decreased at all sites (from >0.41 to <0.38, Supplementary material Fig. S6b). Molecular formulae in DOM_{WE} containing nitrogen ranged between 46 (U1545, 485 mbsf) and 99 % (U1550, 22 mbsf) (Supplementary material Fig. S6c). Molecular formulae of DOM_{WE} containing sulfur ranged between 6 (U1551, 38 mbsf) and 81 % (U1547, 11 mbsf, Supplementary material Fig. S6d). The molecular masses (m/z) decreased from near-surface sediments (from 330 and 345 Da) downcore at all sites (to 266 and 332 Da) (Supplementary Fig. S6f). The intensity-weighted abundance of PCA molecular formulae was highest at Site U1547 at 60 mbsf (~5 %) and approached lowest values at Sites U1545, U1547 and U1550 at the respective deepest samples (Supplementary material Fig. S6h) (the remaining DOM_{WE} groups and parameters are shown in Supplementary material Figs. S6 and S7). Compared to DOM_{PW}, DOM_{WE} was generally less degraded (lower I_{DEG} values), more sulfurized (higher I_{SuP} values), and contained more terrestrial compounds (higher I_{Terr} values) compared to DOM_{PW} (compare Supplementary Fig. S8 to Fig. 4).

Table 2
Bulk geochemical parameters of the two bottom water samples (Alvin dive 4864 from 2 m and dive 4865 from 3 m above ground) compared to the respective shallowest porewater samples at Sites U1545, U1547, U1550, and U1551. The water samples were collected at Site Ringvent during R/V Atlantis cruise AT37-06 (Teske et al., 2019) and are closest to Site U1547.

	Depth [m] or [mbsf][a]	DOC [mM]	TDN [mM]	DON_{SPE} [μM]	C/N_{SPE}	DOS_{SPE} [μM]	C/S_{SPE}	DOP_{SPE} [μM]	C/P_{SPE}
Dive 4864	1725	0.20	1.39	9.5	16	2.7	57	0.05	2902
Dive 4865	1726	0.10	0.21	3.4	16	0.5	115	0.04	1507
U1545	3	0.67	0.53	24	9	7.5	30	0.11	2008
U1547	3	0.44	0.12	18	11	3.6	53	0.11	1728
U1550	3	1.27	1.53	47	13	17	35	0.46	1290
U1551	14	1.06	3.14	13	10	2.1	61	0.12	1128

[a] Water depth in m for samples from dives and sediment depth in mbsf for sediment core samples.

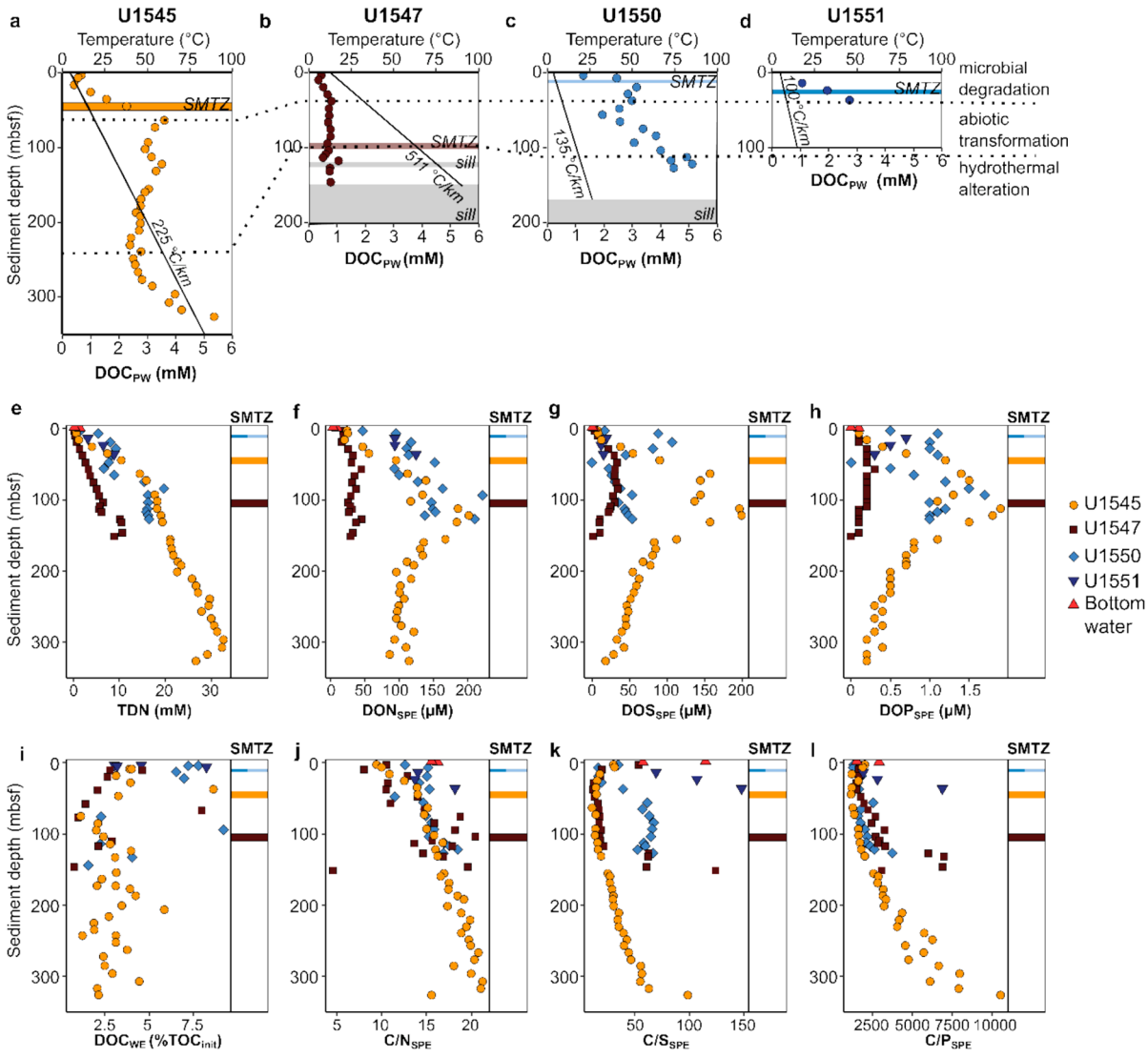

Fig. 2. Profiles of bulk geochemical parameters for DOC_{PW} a) U1545, b) U1547. c) U1550, d) U1551 and e) TDN, f) DON_{SPE}, g) DOS_{SPE}, h) DOP_{SPE}, i) DOC_{WE} (% TOC_{init}), j) C/N_{SPE}, k) C/S_{SPE}, l) C/P_{SPE} over depth for all drilling sites with sulfate-methane transition zones (SMTZ) and temperature data published previously (Teske et al., 2021c–f). Bottom water samples were collected during Alvin dive 4864 from 2 m and dive 4865 from 3 m above ground (R/V Atlantis cruise AT37-06).

3.3. Statistical results

In the PCoA based on the molecular DOM composition of porewater, the first two axes accounted for 69 % of the DOM variability (Fig. 5a). The first axis separated porewater samples by their H/C values, N-containing DOM and NOSC, while the second axis distinguished sites by location and by sulfur-content (DOM containing S and I_{SuP} values) and I_{Terr} values. Deep porewater samples (samples clustering on the right side of PCoA in Fig. 5a) of Sites U1545, U1547 and U1550 were positively correlated with high DOC_{PW} concentrations and unsaturated compounds. Porewater DOM in intermediate depths (samples clustering on the left side of PCoA in Fig. 5a) correlated with high NOSC values, PCA molecular formulae, DOM containing S or P, DOS_{SPE} content, and I_{SuP} and I_{Terr} values. Porewater in upper sediment layers (samples of Sites U1545, U1547, U1551 clustering in the upper left panel of PCoA in Fig. 5a) exhibited high O/C values, higher degradation (I_{DEG}) and high m/z values, high TOC, and CRAM contents and highly unsaturated DOM. Bottom seawater samples clustered with intermediate (U1550) and upper sediment porewater (U1547) or deeper porewater from Sites U1545 and U1547 (Fig. 5a).

In the PCoA of the hot-water Soxhlet-extracted sediments (DOM_{WE}), the first two axes explained 55 % of the DOM molecular variability (Fig. 5b). The first axis separated samples according to highly unsaturated DOM (HUC), DOP_{SPE} content and N-containing DOM, whereas the second axis distinguished sites by sulfur (I_{SuP}) and phosphorus content. The deep sediment samples of Sites U1545 and U1547 were positively correlated with high H/C values, temperature, depth and unsaturated DOM (lower left panel), whereas upper DOM_{WE} samples correlated with NOSC, I_{DEG}, O/C and CRAM values, aromatic and PCA molecular formulae as well as molecular mass (m/z). Sites U1550 and U1551 exhibited higher DOC_{WE} $\%TOC_{init}$ alongside high content of N-containing DOM and I_{Terr} values.

1833 molecular formulae correlated with sediment depth in both DOM_{PW} and DOM_{WE} (Supplementary material Fig. S9). 1409 and 3791 molecular formulae correlated positively or negatively with sediment depth in DOM_{PW} or DOM_{WE} samples exclusively (Fig. 4b, Supplementary material Fig. S9). Relative abundances of molecular formulae positively correlated to sediment depth (red) had H/C values >1 and O/C values <0.3, whereas negatively correlated molecular formulae (blue) had H/C values <1.5 and O/C values >0.3 (Fig. 4b).

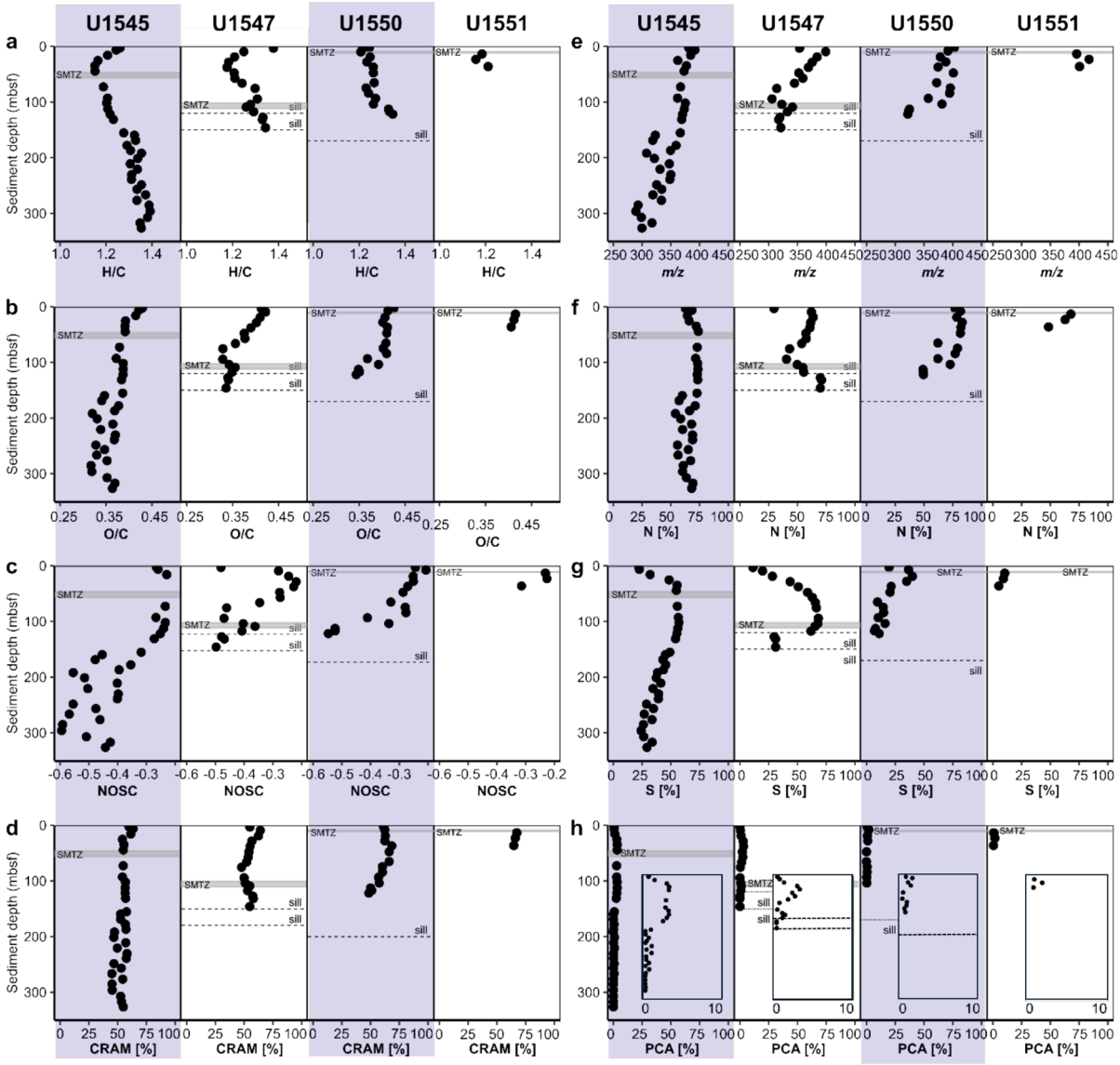

Fig. 3. Profiles of the porewater molecular SPE-DOM composition (DOM_{PW}, from FT-ICR-MS) for the intensity-weighted values of a) H/C, b) O/C, c) NOSC, d) relative abundances of carboxyl-rich alicyclic molecules (CRAM, in %), e) molecular masses (*m/z*), and intensity-weighted relative abundances of molecular formulae containing f) N, g) S, h) polycyclic aromatic (PCA) molecular formulae over depth (in %). Included are enlarged profiles of PCA compounds (0–10 %) for a better visualization of the depth trends. SMTZ, sulfate-methane transition zone.

4. Discussion

Thermal and chemical gradients in the Guaymas Basin create a diverse biogeochemical environment (Teske et al., 2019). This study breaks new ground by venturing into the deep subsurface of Guaymas Basin sediments to investigate how hydrothermal processes shape the DOM_{PW} composition. The reactivity of organic matter in sediments is determined by factors such as age and burial depth, as well as temperature, and microbial activity (Burdige, 1991; Komada et al., 2013; Middelburg, 1989) and therefore, these factors will also influence the amount and composition of DOM_{PW} (Brünjes et al., 2025; Schmidt et al., 2014). These environmental factors also interact in complex ways, making it challenging to determine their individual effects on the persistence of DOM in sediments (Cheng et al., 2024). In the following sections, we will discuss these processes relating them to DOM transformations in the deep subsurface sediments of the Guaymas Basin.

4.1. Biological processes shaping the DOM composition in Guaymas Basin sediments

In the Guaymas Basin, sediments become anoxic after a few centimeters below sediment surface (Teske, 2024). Previous research at our sampling sites has shown that metabolic processes and cellular activity are highest in the upper ~40 mbsf and then drop to near-zero levels at depths >75 mbsf (Mara et al., 2023b). In this microbial active zone (upper sediments <50 mbsf), we observed the lowest DOC_{PW} concentrations in the porewater at all sites (Fig. 2a–d). This is likely due to active microbial communities metabolizing DOM (Bazylinski et al., 1988; Gutierrez et al., 2015) and loss of DOM via diffusion from the near-surface sediments into the ocean (Burdige et al., 1999). DOC concentrations generally increase exponentially with depth in anoxic, organic-rich oceanic margins (Burdige and Komada, 2015) and near-surface hydrothermal sediments (Lin et al., 2017). Therefore, increasing concentrations with depth suggested DOC_{PW} accumulation resulting from an imbalanced release and consumption of DOC (Burdige and Gardner, 1998).

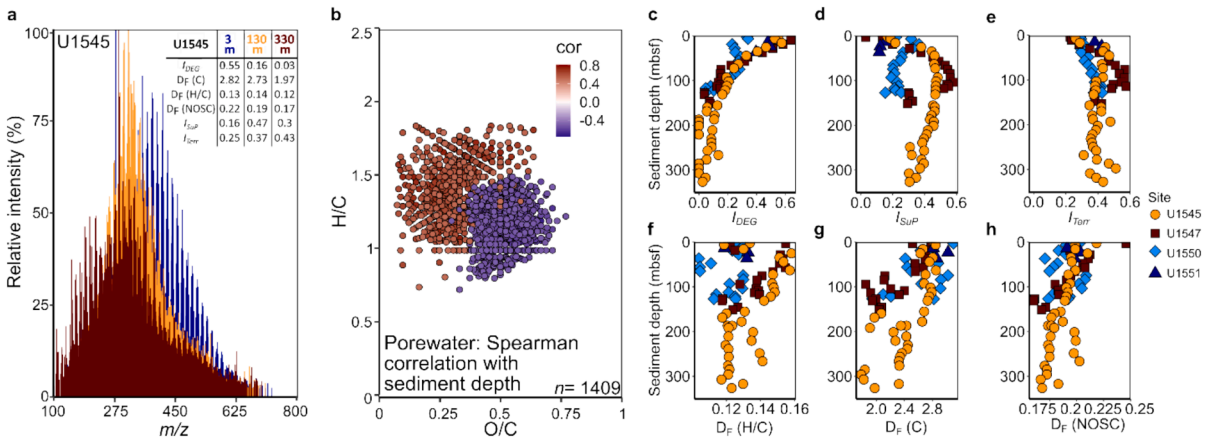

Fig. 4. a) DOM mass spectra of the deepest, intermediate, and shallowest porewater sample from site U1545, b) van-Krevelen plot of DOM_{PW} molecular formulae relative intensities correlated with depth ($\rho > 0.25$, Spearman's correlation), and the molecular indices: c) I_{Deg}, d) I_{SuP}, e) I_{Terr}, and the functional diversity indices (D_F) f) D_F (H/C), g) D_F (C), and h) D_F (NOSC) for the respective sites.

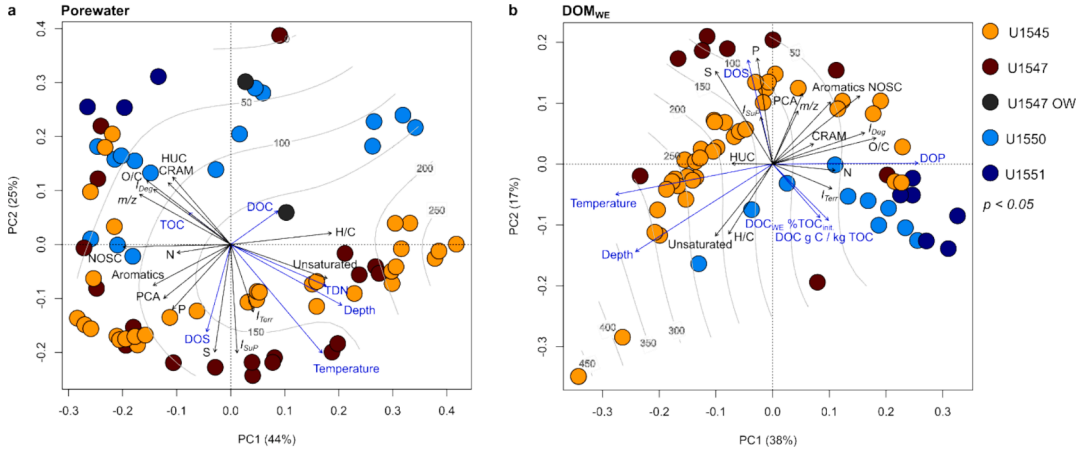

Fig. 5. Principal coordinate analysis (PCoA) based on the relative intensities of all molecular formulae derived from FT-ICR-MS for a) porewater and b) hot water-extractable DOM. Centered and scaled environmental data and intensity-weighted relative abundances of DOM molecular compound groups were fitted to PCoA ordination post hoc (permutations 10,000, $p < 0.05$). Abbreviations: PCA polycyclic aromatic, HUC highly unsaturated compounds, CRAM carboxyl-rich alicyclic molecules, N, S, and P DOM containing nitrogen, sulfur, or phosphorus, OW = overlying water sample near Site U1547. The percentages give the DOM molecular variability as explained by the PC axes; grey isolines represent depth trends.

In the upper ~50 mbsf, DON_{SPE} and DOP_{SPE} concentrations increased with depth, likely due to microbial mobilization from sedimentary organic matter (Schmidt et al., 2009) (Fig. 2f and h). The C/N_{SPE} and C/P_{SPE} values increased only slightly in the upper 50 mbsf, suggesting simultaneous degradation of DOC, DOP_{SPE}, and DON_{SPE} (Fig. 2j and l). Likewise, the pronounced increase of TDN concentrations with depth, especially below the SMTZs at Sites U1545 and U1550 (Fig. 2e), likely resulted from organic matter degradation (Teske et al., 2021c,d), because microbial organic matter remineralization releases inorganic nitrogen, such as ammonium, accumulating under anoxic conditions. At intermediate depths (<100 mbsf), the relative abundances of intensity-weighted N- and P-containing molecular formulae (Fig. 3f, Supplementary Fig. S5a) and bulk concentrations (DON_{SPE} and DOP_{SPE}) remained constant or even increased (Fig. 2f and h). In the microbial active zone (<50 mbsf), the increase of DON_{SPE} and DOP_{SPE} was probably due to protein degradation and release of biomass-derived compounds (Schmidt et al., 2009; Valle et al., 2018). However, at greater depths (>75 mbsf), reduced microbial degradation and increased thermal degradation likely contributed to the accumulation of N- and P- containing DOM (see discussion about hydrothermal DOM alterations below). The increasing C/N_{SPE} and C/P_{SPE} values further suggest a relatively higher release and/or accumulation of DOC_{SPE} compared to DON_{SPE} and DOP_{SPE} indicating a preferential microbial degradation of N- and P-containing DOM with increasing sediment depth.

Porewater DOM in sediments with detectable microbial activity (<70 mbsf) (Mara et al., 2023b) had O/C values >0.4 aligning with previously reported values in marine porewater (Schmidt et al., 2009; Seidel et al., 2014) (Fig. 3b). The D_F values of the molecular DOM parameters in the near-surface sediments were comparable with values reported for relatively young oceanic DOM (less than ~3 years) (Mentges et al., 2017) (Fig. 4f–h). The DOM functional diversity increases with biological transformations (Wang et al., 2021), thus microbial DOM processing may explain the observed higher functional diversity in the upper 50 mbsf compared to deeper sediments. At the same time, the relative increase of PCA molecular formulae with increasing DOC_{PW} concentrations in depths <70 mbsf (PCA in Fig. 3h) may be related to the intrinsic stability of these compounds against microbial degradation (Osterholz et al., 2016; Wagner et al., 2018), leading to a relative accumulation of recalcitrant DOM when labile fractions are consumed.

Active microbial transformations may explain the slightly higher abundances of CRAM in porewater DOM of the upper ~50 mbsf compared to the deeper sections (Fig. 3d), since a net production of

CRAM by microbial communities has been observed during sedimentary organic matter degradation (Fox et al., 2018). CRAM is structurally related to microbial membrane constituents and secondary metabolites, originating from microbial organic matter transformations (Hertkorn et al., 2013). Marine sediments have also been proposed as a source of CRAM to the ocean (Fox et al., 2018). In addition, while seawater diffusion into the sediment might influence the relative abundance of CRAM in the near-subsurface sediments, this influence is likely to be small given the higher DOC concentrations in porewater compared to seawater.

4.2. Abiotic processes dominate the DOM composition in the deep subsurface sediments

At sediment depths >75 mbsf (and temperatures >50 °C), microbial populations and activities are significantly reduced (Mara et al., 2023a; Mara et al., 2023b). In high-temperature sediments (>45 °C), organic substrates become less important when survival conditions become increasingly unfavorable for microbes, limiting microbial diversity and abundance (e.g., at Sites U1545 and U1547) (Mara et al., 2023b). In the mid-section sediments with reduced microbial activity (~50 to ~100 mbsf U1547, U1550, and U1551, or 50–250 mbsf U1545, respectively), decreasing NOSC values with increasing depth reflected the progressive decrease of the DOM oxidation state (Fig. 3c). This trend suggests increasing DOM recalcitrance under anoxic, energy-limited conditions (LaRowe and Van Cappellen, 2011). Hydrothermal petroleum generation releases reduced aliphatic compounds (Simoneit, 2018; Simoneit & Schoell 1995), further contributing to the decreasing NOSC values with depth. In addition, PCA molecular formulae accumulated in intermediate depths (Fig. 3h), probably reflecting the reduced microbial degradation under anoxic conditions and the inherent recalcitrance of their condensed aromatic ring structures (Coppola et al., 2022; Seidel et al., 2014). However, NOSC values also reflect DOM saturation and oxygenation, influencing DOM polarity (Riedel et al., 2012; Stenson, 2008). Oxygen-rich, unsaturated, and condensed aromatic substances exhibit reduced water solubility and may preferentially precipitate with metal phases (Riedel et al., 2012), while the residual, more soluble DOM becomes more saturated and less oxygenated, which is reflected in decreasing NOSC and O/C values with depth (Figs. 3b, c, 4b).

Large parts of the sediments in Guaymas Basin are sulfidic (Supplementary material Fig. S1) (Teske et al., 2021b). In sulfidic sediments, abiotic sulfide incorporation into DOM produces DOS (Pohlabeln et al., 2017). C/S_{SPE} values below 100 and decreasing C/S_{SPE} values towards the SMTZs at Sites U1545, U1547, and U1550 (Fig. 2k) are consistent with DOM sulfurization as a prevalent process (Gomez-Saez et al., 2017; Phillips et al., 2022) producing DOS in the hydrothermal Guaymas Basin sediments. The DOS_{SPE} concentrations peaked near SMTZs aligning with high sulfide concentrations (Fig. 2g). Elevated I_{SuP} (Fig. 4d) and low C/S_{SPE} ratios in depths <50 mbsf (Fig. 2k) further highlight abiotic DOM sulfurization as a significant transformation process at the hydrothermally impacted sites, highlighting the applicability of the I_{SuP} across various sulfidic environments. The C/S_{SPE} values around 11 are amongst the lowest reported values (Gomez-Saez et al., 2021; Gomez-Saez et al., 2016; Ksionzek et al., 2016; Phillips et al., 2022), possibly representing the upper limit of abiotic sulfur incorporation into DOM in sediments.

4.3. Hydrothermal alteration of deep subsurface DOM

Increasing DOC_{PW} concentrations with increasing depth (Fig. 2a–d) likely represent past and recent hydrothermal DOC mobilization from sedimentary organic matter (Lin et al., 2017). Hydrothermal petroleum is generated on geologically short time scales in the Guaymas Basin (Simoneit, 2018). In contrast, in low-organic, high-temperature hydrothermal systems, DOM is highly altered, and most SPE-DOM is removed (Hawkes et al., 2016). Heat-induced fluid flow that follows a sill emplacement diminishes after cooling (Fisher and Narasimhan, 1991). As a result, hydrothermally altered DOC may accumulate in the porewater (Lin et al., 2017). This may explain why DOC_{PW} concentrations were notably lower at the Ringvent Site U1547 (Teske et al., 2019) compared to the other sites. Here, a more recent sill emplacement causes advective transport of fluids toward the overlying water (Neumann et al., 2023). This is also supported by the similarity of the bottom water DOM composition (~2 to 3 m above the ocean floor) and hydrothermally impacted porewater DOM at Site U1547 (clustering of Ringvent bottom seawater with deep porewater samples from Site U1547 in PCoA, Fig. 5a). Therefore, DOC_{PW} concentrations at Site U1547 are possibly lower because of a shorter fluid residence time in the sediments and discharge into the overlying water.

Hydrothermal DOM alteration begins at relatively low temperatures of 68 °C (Hawkes et al., 2016). With increasing depth and temperature, we observed molecular DOM changes, including decreasing molecular masses (m/z), O/C, and NOSC values, along with increasing H/C values in all deep porewater samples from hydrothermally affected Sites U1545, U1547, and U1550 (Fig. 3, Fig. 4). As mentioned above, this reflects hydrothermal petroleum generation, such as the reductive transformation of organic matter (Simoneit, 2018). This process leads to dehydration and decarboxylation, which explains the generally decreasing O/C values (Fig. 3b) and average molecular masses (Fig. 3e) (Hawkes et al., 2016). In addition, the degradation state (I_{DEG}) (Fig. 4c) and functional diversity of porewater SPE-DOM (D_F) decreased at depths approaching sill intrusions (i.e., our deepest samples, Fig. 4f–h). This pattern suggests thermally altered, but microbially unprocessed DOM (Hansen et al., 2019; Lin et al., 2017), which accumulates when high sediment temperatures inhibit microbial degradation. Due to the severely reduced microbial abundances at temperatures above 50 to 60 °C (Mara et al., 2023a), deep subsurface sediments accumulate DOM until thermal degradation occurs. However, the interplay of DOM thermal degradation and DOM bioavailability is highly complex, which is evident when considering the fate of reduced aliphatic compounds such as alkanes. While reduced petroleum compounds with low NOSC values such as alkanes, are energetically less favorable substrates than oxidized compounds, specialized alkane-degrading microbes are generally able to utilize this compound group in sediments <75 mbsf and at <50 °C (Mara et al., 2022; Ramírez et al., 2021; Teske et al., 2014).

Increasing DOC_{PW} concentrations with depth, along with decreasing DOS_{SPE}, DON_{SPE}, and DOP_{SPE} concentrations, suggest that hydrothermal transformations may favor the release of DOC into porewater. Sulfur and phosphorus compounds are both generated and degraded during these hydrothermal processes (Hawkes et al 2016). While sulfur compounds are mostly removed during thermal degradation at temperature >100 °C, new sulfur compounds can also form at various temperatures (Hawkes et al., 2016), especially under sulfidic conditions (Gomez-Saez et al., 2016). During thermal alteration, nitrogen-containing DOM can undergo decarboxylation, dehydration, and ring-closure, potentially forming dissolved black nitrogen and dissolved black carbon in thermal environments (Hawkes et al., 2016). The observed DON_{SPE} and DOP_{SPE} concentrations can be explained by thermal degradation, which release inorganic constituents such as ammonium and phosphate through deamination and dephosphorylation (Moeller et al., 2022; Robinson et al., 2019). This is consistent with the observed increase of ammonium and TDN concentrations with depth (Fig. 2e, Supplementary Fig. S1). As microbial activity declines in deeper, high temperature sediments (>60 °C), thermal degradation processes become more dominant, in contrast to the upper ~50 mbsf characterized by high microbial activity.

4.4. Hydrothermal circulation mobilizes deep subsurface DOM

The stable carbon isotopic composition ($\delta^{13}C$) of porewater and water-extractable SPE-DOM exhibited values typical for marine SPE-DOM (around −23 ‰, Supplementary material Fig. S4), reflecting

dominant marine (algal) organic matter sources in Guaymas Basin sediments (Teske et al., 2021b). In line with this, petroleum in Guaymas Basin sediments is generated from marine sedimentary kerogen (Simoneit and Schoell, 1995). At the southern Site U1551 (Fig. 1), $\delta^{13}C$ SPE-DOM values were more negative (Supplementary material Fig. S4), likely because of terrigenous input from the Yaqui River in that region (Teske et al., 2021b), which was also observed in the sediment composition gradient from north to south in the Guaymas Basin (Persad and Marsaglia, 2023).

Porewater SPE-DOM (DOM_{PW}) exhibited significantly more negative $\delta^{13}C$ values compared to hydrothermally mobilizable DOM_{WE} ($p = 2.89 \times 10^{-5}$, Wilcoxon–Whitney test), suggesting a greater terrestrial contribution in porewater than in DOM_{WE} (Supplementary material Fig. S4). This may indicate that sorption to sediment mineral phases preserves marine organic matter (less negative $\delta^{13}C$ values) from degradation (Guggenberger and Kaiser, 2003; Keil et al., 1994), whereas marine DOM in the porewater may have been more degradable than the terrestrial DOM (more negative $\delta^{13}C$ values) (Fu et al., 2022).

The molecular compositions of DOM_{PW} and DOM_{WE} were distinctly different, as evidenced by variations in degradation (I_{DEG}), sulfurization (I_{SuP}), and terrestrial DOM (I_{Terr}) indices. Notably, DOM_{WE} was generally less degraded (lower I_{DEG} values), more sulfurized (higher I_{SuP}), and contained more terrestrial compounds (higher I_{Terr} values) compared to DOM_{PW} (Supplementary Fig. S8, Fig. 4). However, the higher I_{Terr} values in DOM_{WE}, indicating a greater abundance of terrestrial compounds compared to DOM_{PW}, contrast with the $\delta^{13}C$ SPE-DOM values, which were more negative in DOM_{PW} than in DOM_{WE} (Supplementary Fig. S4). This suggests that the differences in $\delta^{13}C$ SPE-DOM values between DOM_{WE} and DOM_{PW} are likely driven by varying degradation states of specific organic compound classes rather than solely by terrestrial input. Lipids, proteins, or carbohydrates may be degraded at different rates, leading to the degradation of more bioavailable compounds and preservation of more recalcitrant compounds, such as lipids (Hatcher et al., 1983). Water-extractable DOM (DOM_{WE}) also appears to consist of a fresher, less degraded DOM, compared to more degraded porewater DOM (Schmidt et al., 2014). Selective degradation of isotopically heavier compounds, such as carbohydrates and proteins (van Dongen et al., 2002) may therefore explain the more negative $\delta^{13}C$ SPE-DOM values in DOM_{PW} compared to DOM_{WE}, the latter potentially containing preserved, isotopically heavier compounds such as protein-derived material.

Despite these compositional differences, both DOM_{WE} and DOM_{PW} exhibited comparable depth-related trends, including decreasing I_{DEG} values with depth, and elevated I_{SuP} values in intermediate depths (near the SMTZs). This indicates that while their molecular compositions differ, the dominant biogeochemical processes such as microbial degradation, sulfurization, and hydrothermal degradation affect both pools comparably along sediment depth gradients. Furthermore, the difference of $\delta^{13}C$ values between DOM_{PW} and mobilizable DOM_{WE} indicated that hydrothermal circulation through sediments potentially mobilizes DOM which is more readily degradable compared to porewater DOM. Another possible explanation for the depleted $\delta^{13}C$ DOM_{PW} values is DOC derived from microbial biomass of microbes using methane as carbon source which is generally strongly depleted in ^{13}C (Hu et al., 2021).

We followed the approach by Lin et al. (2017) to test the mobilization of DOC_{WE} from sediments via hot-water fluid flow using Soxhlet extraction. Our results showed that deeper sediments with hydrothermally altered organic matter had a lower proportion of total sedimentary organic carbon (TOC) that is water extractable as DOC (i.e., lower DOC_{WE} $\%TOC_{init}$ values), compared to shallow sediments containing relatively young and less degraded organic matter (Fig. 2i). This suggests that thermal alteration of the deeper sediments reduced the content of water-extractable DOC and as such the potential for carbon mobilization via advective fluid flow. This is consistent with previous observations in Guaymas Basin where hot, hydrothermally-altered surface sediments contained less water-extractable DOC than cooler sediments (Lin et al., 2017). At Sites U1545 and U1547, where higher temperature gradients were observed, the reduced DOC_{WE} $\%TOC_{init}$ values indicated that advective fluid flow has likely altered the composition of sedimentary organic matter and porewater DOM, even if current hydrothermal activity has stopped (Neumann et al., 2023). The molecular DOM composition of DOM_{WE} and DOM_{PW} exhibited comparable trends with sediment depth. For example, samples from depths >200 mbsf were associated with high abundances of unsaturated DOM, whereas shallower samples correlated with high O/C values in both water-extractable and porewater DOM (Fig. 5). These consistent trends between DOM_{WE} and DOM_{PW} suggest that aqueous Soxhlet extraction is a promising complementary approach for organic matter analyses, especially when porewater availability is limited (Lin et al., 2017; Schmidt et al., 2014).

Soxhlet extraction provides valuable insights into DOM_{WE} dynamics and composition (Lin et al., 2017; Schmidt et al., 2014), but it remains a simplified proxy for hydrothermal mobilization. Our ultrapure-water extractions were conducted under anoxic conditions, using wet sediments containing porewater, which increased salinity and matched the lower range of the natural pH values (7.0–8.2). However, this approach does not fully replicate in-situ hydrothermal conditions where variations of salinity, hydrostatic pressure, and redox conditions occur on geological timescales. Additionally, Soxhlet extraction was performed at ~100 °C under atmospheric pressure, whereas hydrothermal fluids in Guaymas Basin range from ~4 °C to >300 °C, potentially affecting DOM solubility, transformations, and mobilization potential of specific compounds. Despite these limitations, our controlled approach provides key insights into DOM hydrothermal mobilization. Thus, Soxhlet extraction should be viewed as a first-order approximation that complements, rather than directly simulates, natural hydrothermal processes (Lin et al., 2017).

To compare relative DOM compound group abundances between porewater and water-extractable samples, we used normalized data (scaled between 0 and 1) based on intensity-weighted relative abundances and DOC concentrations (using DOC_{PW}* and DOC_{WE}*). Our results indicated a higher potential for hydrothermal DOM mobilization in the central and southern Guaymas Basin Sites U1550 and U1551, which had higher DOC_{WE}* values compared to DOC_{PW}* and which showed higher relative abundances of all DOM compound classes than the other sites (Supplementary material Fig. S10). In addition, differences in lithology between sites with hot/moderate temperature gradients and cooler sites probably contribute to varying hydrothermal carbon mobilization potentials. Sediments from Sites U1545 and U1547 are primarily marine (diatom ooze and clay), whereas sediments at Sites U1550 and U1551 have a higher terrigenous input (silt and clay) (Persad and Marsaglia, 2023). Hence, the higher hydrothermal carbon mobilization potential at these two sites appears to result from both sediment composition and potentially lower hydrothermal alteration.

4.5. Hydrothermal DOM transport to the ocean

Diffusion of porewater from marine sediments is an important source of DOC and DON to the ocean (Burdige and Komada, 2015). However, the contribution of sedimentary fluxes to the global oceanic DON and DOP pools is still not well understood (Burdige and Komada, 2015). In the Guaymas Basin, porewater discharge and diffusion probably contribute DON_{SPE} and DOP_{SPE} to near-bottom waters. This was supported by lower C/N_{SPE} (16) and C/P_{SPE} (1507 and 2902) values in bottom water DOM collected above our study sites (Table 2) compared to non-hydrothermally affected seawater DOM ($C/N_{SPE} > 20$, $C/P_{SPE} > 2200$) (Ksionzek et al., 2018). Additionally, the molecular DOM composition of shallow subsurface porewater and bottom seawater (2 to 3 m above sediment surface) indicated a lower degree of degradation (I_{DEG} 0.33–0.64, Fig. 4c, 0.45 and 0.69, respectively, Supplementary Table S2) compared to deep-sea DOM elsewhere ($I_{DEG} > 0.75$, Atlantic

Ocean) (Flerus et al., 2012). These results emphasize the role of benthic DOM fluxes in transporting DOM to the overlying water.

DOM fluxes are not only driven by diffusion, but also vertical fluid upwelling (up to 8 m kyr^{-1} at Site U1545 in <500 mbsf) (Sarkar et al., 2022), and sediment compaction, leading to a DOC efflux of 27 Gg C yr^{-1} in the Guaymas Basin (Lin et al., 2017). Globally, sulfidic sediments contribute 8 to 39 % of oceanic DOS_{SPE} (Ibrahim and Tremblay, 2023; Phillips et al., 2022). In the Guaymas Basin bottom water, elevated DOS_{SPE} concentrations (0.5 μM and 2.7 μM) and lower C/S_{SPE} values (57 and 115, near Ringvent Site U1547) (Table 2) compared with the deep Pacific Ocean (DOS_{SPE} 0.16 μM, C/S_{SPE} 250) (Phillips et al., 2022) indicated benthic DOS_{SPE} fluxes to the ocean. Thus, our data support the assumption that sulfidic hydrothermal systems are important contributors to the oceanic DOS pool (Gomez-Saez et al., 2016).

Future shallow magmatic emplacements in the study area might mobilize and release large volumes of sedimentary carbon, for example via outgassing of methane and CO_2 (Lizarralde et al., 2011). Our simplified hydrothermal mobilization experiments using hot-water Soxhlet extractions suggest that unaltered and altered sediments have the potential to release DOM. Consistent with previous studies, our findings suggest that hydrothermal heating can mobilize DOM, indicating that fossil and previously stable organic deposits may be remobilized by sill emplacements (Lin et al., 2017; Lizarralde et al., 2011; Lizarralde et al., 2023). Sediments generally release recalcitrant and labile DOM (Fejjar et al., 2021), including marine DOS (Ibrahim and Tremblay, 2023). Our data indicate that hydrothermal alteration can influence the release of DOM from sediments, with hydrothermal DOM discharge to the deep sea. This process may not only alter bottom water chemistry (Lin et al., 2017) but could also have broader implications for the deep-sea carbon cycle through the export of DOM, including DOS.

5. Conclusions

Our study highlights DOM dynamics in hydrothermally altered, organic-rich subsurface sediments. Trends in DOM composition indicate that microbial processes influenced the porewater DOM composition in the shallow microbial active zones. Abiotic processes, on the other hand, like DOM sulfurization, played a significant role in deeper, less microbially active sediments. Furthermore, DOM accumulated with sediment depth, presumably due to decreasing microbial activities at increasing temperatures. Hydrothermal alteration strongly influenced the DOM composition in sediments adjacent to sill intrusions.

Our laboratory experiments using hot-water Soxhlet extraction indicated potential for carbon mobilization via hot-water advective fluid transport, which decreased with higher hydrothermal alteration of the sediments. In contrast to previous work, our study considers sediments and porewater beyond the sediment surface of ocean margins and reveals that DOM persists in the deep subsurface. However, when active sill emplacement alters sedimentary organic matter, advective fluid transport is a source of DOM to the ocean, including DOS_{SPE}, DON_{SPE} and DOP_{SPE}, that enters the overlying water at the Ringvent Site. Hence, hydrothermal discharge not only sustains local benthic ecosystems by providing bioavailable hydrocarbons but also has the potential to influence the deep-sea carbon pool by introducing recalcitrant DOM, including DOS_{SPE}. We further conclude that hydrothermal activity in organic-rich systems can disrupt sedimentary carbon storage by actively remobilizing DOM.

Author contributions

M. K. and J.G. processed samples. A.T. provided samples. M. K. analyzed data and performed statistical analyses. M.S., T.D., A.T., J. G. and P.B. contributed significantly to data interpretation. M.K. and M.S. wrote the manuscript with significant input from all co-authors. All authors reviewed and approved the final manuscript.

Data availability

The data collected during this research are available via PANGAEA at: https://doi.pangaea.de/10.1594/PANGAEA.974052.

CRediT authorship contribution statement

Melina Knoke: Writing – review & editing, Writing – original draft, Visualization, Investigation, Formal analysis, Data curation, Conceptualization. **Thorsten Dittmar:** Writing – review & editing, Writing – original draft, Supervision, Investigation, Conceptualization. **Jana Günther:** Writing – review & editing, Investigation, Formal analysis. **Philipp Böning:** Writing – review & editing, Methodology, Investigation. **Andreas Teske:** Writing – review & editing, Supervision, Investigation, Conceptualization. **Michael Seidel:** Writing – review & editing, Writing – original draft, Supervision, Methodology, Investigation, Funding acquisition, Conceptualization.

Declaration of competing interest

The authors declare that they have no known competing financial interests or personal relationships that could have appeared to influence the work reported in this paper.

Acknowledgements

This research used samples and data provided by the International Ocean Discovery Program (IODP) Expedition 385. Funding for this research was provided by Deutsche Forschungsgemeinschaft (DFG) SPP 527 “International Ocean Discovery Program” (IODP) (Project number 447583997) and DFG Cluster of Excellence EXC2077 “The Ocean Floor – Earth’s Uncharted Interface” (project number 390741603). We thank the scientists and crew of Expedition 385 on the JOIDES Resolution. We appreciate the technical support of Eleonore Gründken, Ina Ulber, Katrin Klaproth, Heike Simon, and Matthias Friebe in the laboratories at ICBM. We further thank Dr. Florence Schubotz, Dr. Kai-Uwe Hinrichs, and Dr. Jonas Brünjes for providing the Soxhlet apparatus and valuable scientific discussions. We thank Dr. Bert Engelen for his scientific support in conducting this study.

Appendix A. Supplementary material

The Supplementary Material includes additional method descriptions, 10 Figures, 2 Tables, and references. Figures present (1) depth profiles of TOC, sulfate, sulfide, and ammonium, (2) porewater sulfate and methane concentrations, (3) DOC* calculation diagram, (4) $\delta^{13}C$ depth profiles of porewater (DOMPW) and hot water-extractable SPE-DOM (DOMWE), (5) molecular parameters of DOMPW, (6) molecular parameters of water-extractable DOMWE, (7) NOSC and CRAM depth profiles in DOMWE, (8) molecular indices of DOMWE, (9) density and van-Krevelen plots correlating molecular formulae intensities with sediment depth, and (10) depth profiles of SPE-DOM compound groups in porewater (DOMPW*) and water-extractable DOM (DOMWE*). Tables provide details on DOM extraction conditions and molecular parameters of water column SPE-DOM. Supplementary material to this article can be found online at https://doi.org/10.1016/j.gca.2025.06.005.

References

Abdulla, H.A., Burdige, D.J., Komada, T., 2020. Abiotic formation of dissolved organic sulfur in anoxic sediments of Santa Barbara Basin. Org. Geochem. 139, 103879.

Bazylinski, D.A., Farrington, J.W., Jannasch, H.W., 1988. Hydrocarbons in surface sediments from a Guaymas Basin hydrothermal vent site. Org. Geochem. 12, 547–558.

Benjamini, Y., Hochberg, Y., 1995. Controlling the false discovery rate: a practical and powerful approach to multiple testing. J. Roy. Stat. Soc.: Ser. B (Methodol.) 57, 289–300.
Bojanova, D.P., De Anda, V.Y., Haghnegahdar, M.A., Teske, A.P., Ash, J.L., Young, E.D., Baker, B.J., LaRowe, D.E., Amend, J.P., 2023. Well-hidden methanogenesis in deep, organic-rich sediments of Guaymas Basin. ISME J 17, 1828–1838.
Brünjes, J., Schubotz, F., Teske, A., Seidel, M., 2025. Molecular composition of dissolved organic matter from young organic-rich hydrothermal deep-sea sediments. Limnol. Oceanogr. 70, 870–885.
Burdige, D.J., 1991. The kinetics of organic matter mineralization in anoxic marine sediments. J. Mar. Res. 49.
Burdige, D.J., Berelson, W.M., Coale, K.H., McManus, J., Johnson, K.S., 1999. Fluxes of dissolved organic carbon from California continental margin sediments. Geochim. Cosmochim. Acta 63, 1507–1515.
Burdige, D.J., Gardner, K.G., 1998. Molecular weight distribution of dissolved organic carbon in marine sediment pore waters. Mar. Chem. 62, 45–64.
Burdige, D.J., Komada, T., 2015. Sediment pore waters. In: Biogeochemistry of Marine Dissolved Organic Matter. Elsevier, pp. 535–577.
Calvert, S.E., 1966. Origin of diatom-rich, varved sediments from the Gulf of California. J. Geol. 74, 546–565.
Cheng, Y., Ding, S., Shao, Z., Song, D., Jiao, L., Zhang, W., Duan, P., He, J., 2024. Persistence of dissolved organic matter in sediments influenced by environmental factors: implication for nutrition and carbon cycle. J. Environ. Manage. 363, 121387.
Coppola, A.I., Wagner, S., Lennartz, S.T., Seidel, M., Ward, N.D., Dittmar, T., Santín, C., Jones, M.W., 2022. The black carbon cycle and its role in the Earth system. Nat. Rev. Earth Environ. 3, 516–532.
Curray, J.R., Moore, D.G., Aguayo, J.E., Aubry, M.P., Einsele, G., Fornari, D.J., Gieskes, J., Guerrero, J.C., Kastner, M., Kelts, K., Lyle, M., Matoba, Y., Mollina-Cruz, A., Niemitz, J., Rueda, J., Saunders, A.D., Schrader, H., Simoneit, B.R.T., Vacquier, V., 1982. Initial Reports of the Deep Sea Drilling Project, 64: 1313 pp.
Damsté, J.S.S., Rijpstra, W.I.C., Kock-van Dalen, A., De Leeuw, J.W., Schenck, P., 1989. Quenching of labile functionalised lipids by inorganic sulphur species: evidence for the formation of sedimentary organic sulphur compounds at the early stages of diagenesis. Geochim. Cosmochim. Acta 53, 1343–1355.
Dittmar, T., Koch, B., Hertkorn, N., Kattner, G., 2008. A simple and efficient method for the solid-phase extraction of dissolved organic matter (SPE-DOM) from seawater. Limnol. Oceanogr. Methods 6, 230–235.
Dittmar, T., Lennartz, S.T., Buck-Wiese, H., Hansell, D.A., Santinelli, C., Vanni, C., Blasius, B., Hehemann, J.-H., 2021. Enigmatic persistence of dissolved organic matter in the ocean. Nat. Rev. Earth Environ. 2, 570–583.
Edgcomb, V.P., Teske, A.P., Mara, P., 2022. Microbial Hydrocarbon Degradation in Guaymas Basin—Exploring the Roles and potential Interactions of Fungi and Sulfate-reducing Bacteria. Front. Microbiol. 13, 831828.
Fejjar, S., Melanson, A., Tremblay, L., 2021. Pore waters as a contributor to deep-water amino acids and to deep-water dissolved organic matter concentration and composition in estuarine and marine waters. Mar. Chem. 233, 103985.
Fisher, A.T., Narasimhan, T.N., 1991. Numerical simulations of hydrothermal circulation resulting from basalt intrusions in a buried spreading center. Earth Planet. Sci. Lett. 103, 100–115.
Flerus, R., Lechtenfeld, O.J., Koch, B.P., McCallister, S.L., Schmitt-Kopplin, P., Benner, R., Kaiser, K., Kattner, G., 2012. A molecular perspective on the ageing of marine dissolved organic matter. Biogeosciences 9, 1935–1955.
Fox, C.A., Abdulla, H.A., Burdige, D.J., Lewicki, J.P., Komada, T., 2018. Composition of dissolved organic matter in pore waters of anoxic marine sediments analyzed by 1H nuclear magnetic resonance spectroscopy. Front. Mar. Sci. 5.
Fu, W., Xu, X., Druffel, E.M., Wang, X., Sun, S., Luo, C., Zhang, H., Fan, D., 2022. Carbon isotopic constraints on the degradation and sequestration of organic matter in river-influenced marginal sea sediments. Limnol. Oceanogr. 67, S61–S75.
Gomez-Saez, G.V., Dittmar, T., Holtappels, M., Pohlabeln, A.M., Lichtschlag, A., Schnetger, B., Boetius, A., Niggemann, J., 2021. Sulfurization of dissolved organic matter in the anoxic water column of the Black Sea. Sci. Adv. 7, eabf6199.
Gomez-Saez, G.V., Niggemann, J., Dittmar, T., Pohlabeln, A.M., Lang, S.Q., Noowong, A., Pichler, T., Wörmer, L., Bühring, S.I., 2016. Molecular evidence for abiotic sulfurization of dissolved organic matter in marine shallow hydrothermal systems. Geochim. Cosmochim. Acta 190, 35–52.
Gomez-Saez, G.V., Pohlabeln, A.M., Stubbins, A., Marsay, C.M., Dittmar, T., 2017. Photochemical alteration of dissolved organic sulfur from sulfidic porewater. Environ. Sci. Technol. 51, 14144–14154.
Green, N.W., Perdue, E.M., Aiken, G.R., Butler, K.D., Chen, H., Dittmar, T., Niggemann, J., Stubbins, A., 2014. An intercomparison of three methods for the large-scale isolation of oceanic dissolved organic matter. Mar. Chem. 161, 14–19.
Guggenberger, G., Kaiser, K., 2003. Dissolved organic matter in soil: challenging the paradigm of sorptive preservation. Geoderma 113, 293–310.
Gutierrez, T., Biddle, J.F., Teske, A., Aitken, M.D., 2015. Cultivation-dependent and cultivation-independent characterization of hydrocarbon-degrading bacteria in Guaymas Basin sediments. Front. Microbiol. 6, 695.
Hansen, C.T., Niggemann, J., Giebel, H.-A., Simon, M., Bach, W., Dittmar, T., 2019. Biodegradability of hydrothermally altered deep-sea dissolved organic matter. Mar. Chem. 217, 103706.
Hatcher, P.G., Spiker, E.C., Szeverenyi, N.M., Maciel, G.E., 1983. Selective preservation and origin of petroleum-forming aquatic kerogen. Nature 305, 498–501.
Hawkes, J.A., Hansen, C.T., Goldhammer, T., Bach, W., Dittmar, T., 2016. Molecular alteration of marine dissolved organic matter under experimental hydrothermal conditions. Geochim. Cosmochim. Acta 175, 68–85.
Hawkes, J.A., Rossel, P.E., Stubbins, A., Butterfield, D., Connelly, D.P., Achterberg, E.P., Koschinsky, A., Chavagnac, V., Hansen, C.T., Bach, W., Dittmar, T., 2015. Efficient removal of recalcitrant deep-ocean dissolved organic matter during hydrothermal circulation. Nat. Geosci. 8, 856–860.
Hertkorn, N., Harir, M., Koch, B.P., Michalke, B., Schmitt-Kopplin, P., 2013. High-field NMR spectroscopy and FTICR mass spectrometry: powerful discovery tools for the molecular level characterization of marine dissolved organic matter. Biogeosciences 10, 1583–1624.
Hu, T., Luo, M., Xu, Y., Gong, S., Chen, D., 2021. Production of labile protein-like dissolved organic carbon associated with anaerobic methane oxidization in the Haima Cold Seeps, South China Sea. Front. Mar. Sci. 8.
Ibrahim, H., Tremblay, L., 2023. Origin of dissolved organic sulfur in marine waters and the impact of abiotic sulfurization on its composition and fate. Mar. Chem., 104273
Kawka, O.E., Simoneit, B.R., 1987. Survey of hydrothermally-generated petroleums from the Guaymas Basin spreading center. Org Geochem. 11, 311–328.
Keil, R.G., Montluçon, D.B., Prahl, F.G., Hedges, J.I., 1994. Sorptive preservation of labile organic matter in marine sediments. Nature 370, 549–552.
Knoke, M., Dittmar, T., Zielinski, O., Kida, M., Asp, N.E., de Rezende, C.E., Schnetger, B., Seidel, M., 2024. Outwelling of reduced porewater drives the biogeochemistry of dissolved organic matter and trace metals in a major mangrove-fringed estuary in Amazonia. Limnol. Oceanogr. 69, 262–278.
Koch, B.P., Dittmar, T., 2006. From mass to structure: an aromaticity index for high-resolution mass data of natural organic matter. Rapid Commun. Mass Spectrom. 20, 926–932.
Koch, B.P., Dittmar, T., 2016. From mass to structure: an aromaticity index for high-resolution mass data of natural organic matter. Rapid Commun. Mass Spectrom. 30, 250.
Kolawole, F., Evenick, J.C., 2023. Global distribution of geothermal gradients in sedimentary basins. Geosci. Front. 14, 101685.
Komada, T., Burdige, D.J., Crispo, S.M., Druffel, E.R., Griffin, S., Johnson, L., Le, D., 2013. Dissolved organic carbon dynamics in anaerobic sediments of the Santa Monica Basin. Geochim. Cosmochim. Acta 110, 253–273.
Ksionzek, K.B., Lechtenfeld, O.J., McCallister, S.L., Schmitt-Kopplin, P., Geuer, J.K., Geibert, W., Koch, B.P., 2016. Dissolved organic sulfur in the ocean: biogeochemistry of a petagram inventory. Science 354, 456–459.
Ksionzek, K.B., Zhang, J., Ludwichowski, K.-U., Wilhelms-Dick, D., Trimborn, S., Jendrossek, T., Kattner, G., Koch, B.P., 2018. Stoichiometry, polarity, and organometallics in solid-phase extracted dissolved organic matter of the Elbe-Weser estuary. PLoS One 13, e0203260.
LaRowe, D.E., Van Cappellen, P., 2011. Degradation of natural organic matter: a thermodynamic analysis. Geochim. Cosmochim. Acta 75, 2030–2042.
Lin, Y.-S., Koch, B.P., Feseker, T., Ziervogel, K., Goldhammer, T., Schmidt, F., Witt, M., Kellermann, M.Y., Zabel, M., Teske, A., 2017. Near-surface heating of young rift sediment causes mass production and discharge of reactive dissolved organic matter. Sci. Rep. 7, 44864.
Lizarralde, D., Axen, G.J., Brown, H.E., Fletcher, J.M., González-Fernández, A., Harding, A.J., Holbrook, W.S., Kent, G.M., Paramo, P., Sutherland, F., Umhoefer, P. J., 2007. Variation in styles of rifting in the Gulf of California. Nature 448, 466–469.
Lizarralde, D., Soule, S.A., Seewald, J.S., Proskurowski, G., 2011. Carbon release by off-axis magmatism in a young sedimented spreading centre. Nat. Geosci. 4, 50–54.
Lizarralde D, Teske A, Höfig TW, González-Fernández A, Scientists tIE (2023) Carbon released by sill intrusion into young sediments measured through scientific drilling. Geology, 51: 329-333.
Mara, P., Geller-McGrath, D., Edgcomb, V., Beaudoin, D., Morono, Y., Teske, A., 2023a. Metagenomic profiles of archaea and bacteria within thermal and geochemical gradients of the Guaymas Basin deep subsurface. Nat. Commun. 14, 7768.
Mara, P., Nelson, R.K., Reddy, C.M., Teske, A., Edgcomb, V.P., 2022. Sterane and hopane biomarkers capture microbial transformations of complex hydrocarbons in young hydrothermal Guaymas Basin sediments. Commun. Earth Environ. 3, 250.
Mara, P., Teske, A.P., Edgcomb, V.P., 2024. Data report: hydrocarbon profiles of selected IODP Expedition 385 Guaymas Basin samples and comparison to shallow surficial push core samples from AT42-05. In: Teske, A., Lizarralde, D., Höfig, T.W., and the Expedition 385 Scientists, Guaymas Basin Tectonics and Biosphere. Proceedings of the International Ocean Discovery Program, 385: College Station, TX (International Ocean Discovery Program). https://doi.org/10.14379/iodp.proc.385.205.2024.
Mara, P., Zhou, Y.-L., Teske, A., Morono, Y., Beaudoin, D., Edgcomb, V., 2023b. Microbial gene expression in Guaymas Basin subsurface sediments responds to hydrothermal stress and energy limitation. ISME J. 17, 1907–1919.
Medeiros, P.M., Seidel, M., Niggemann, J., Spencer, R.G.M., Hernes, P.J., Yager, P.L., Miller, W.L., Dittmar, T., Hansell, D.A., 2016. A novel molecular approach for tracing terrigenous dissolved organic matter into the deep ocean. Global Biogeochem. Cycles 30, 689–699.
Mentges, A., Feenders, C., Seibt, M., Blasius, B., Dittmar, T., 2017. Functional molecular diversity of marine dissolved organic matter is reduced during degradation. Front. Mar. Sci. 4, 194.
Merder, J., Freund, J.A., Feudel, U., Hansen, C.T., Hawkes, J.A., Jacob, B., Klaproth, K., Niggemann, J., Noriega-Ortega, B.E., Osterholz, H., Rossel, P.E., Seidel, M., Singer, G., Stubbins, A., Waska, H., Dittmar, T., 2020. ICBM-OCEAN: processing ultrahigh-resolution mass spectrometry data of complex molecular mixtures. Anal. Chem. 92 (10), 6832–6838.
Middelburg, J.J., 1989. A simple rate model for organic matter decomposition in marine sediments. Geochim. Cosmochim. Acta 53, 1577–1581.
Moeller, C., Schmidt, C., Guyot, F., Wilke, M., 2022. Hydrolysis rate constants of ATP determined in situ at elevated temperatures. Biophys. Chem. 290, 106878.
Neumann, F., Negrete-Aranda, R., Harris, R.N., Contreras, J., Galerne, C.Y., Peña-Salinas, M.S., Spelz, R.M., Teske, A., Lizarralde, D., Höfig, T.W., Scientists, E., 2023. Heat flow and thermal regime in the Guaymas Basin, Gulf of California: estimates of conductive and advective heat transport. Basin Res. 35, 1308–1328.

Oksanen, J., Simpson, G., Blanchet, F., Kindt, R., Legendre, P., Minchin, P., O'Hara, R., Solymos, P., Stevens, M., Szoecs, E., Wagner, H., Barbour, M., Bedward, M., Bolker, B., Borcard, D., Carvalho, G., Chirico, M., De Caceres, M., Durand, S., Evangelista, H., FitzJohn, R., Friendly, M., Furneaux, B., Hannigan, G., Hill, M., Lahti, L., McGlinn, D., Ouellette, M., Ribeiro Cunha, E., Smith, T., Stier, A., Ter Braak, C., Weedon, J., 2022. vegan community ecology package version 2.6-4.

Osterholz, H., Kirchman, D.L., Niggemann, J., Dittmar, T., 2016. Environmental drivers of dissolved organic matter molecular composition in the Delaware estuary. Front. Earth Sci. 4, 95.

Persad, L.D., Marsaglia, K.M., 2023. Data report: Detailed Lithologic Columns for IODP Expedition 385 and DSDP Leg 64 sites in the Guaymas Basin, Gulf of California, Mexico. In: Teske, A., Lizarralde, D., Höfig, T.W., and the Expedition 385 Scientists, Guaymas Basin Tectonics and Biosphere. Proceedings of the International Ocean Discovery Program, 385: College Station, TX (International Ocean Discovery Program). https://doi.org/10.14379/iodp.proc.385.202.2023.

Phillips, A.A., White, M.E., Seidel, M., Wu, F., Pavia, F.F., Kemeny, P.C., Ma, A.C., Aluwihare, L.I., Dittmar, T., Sessions, A.L., 2022. Novel sulfur isotope analyses constrain sulfurized porewater fluxes as a minor component of marine dissolved organic matter. Proc. Natl. Acad. Sci. 119, e2209152119.

Pohlabeln, A.M., Dittmar, T., 2015. Novel insights into the molecular structure of non-volatile marine dissolved organic sulfur. Mar. Chem. 168, 86–94.

Pohlabeln, A.M., Gomez-Saez, G.V., Noriega-Ortega, B.E., Dittmar, T., 2017. Experimental evidence for abiotic sulfurization of marine dissolved organic matter. Front. Mar. Sci. 4, 364.

R Core Team, 2023. R: A Language and Environment for Statistical Computing. R Foundation for Statistical Computing, Vienna, Austria.

Ramírez, G.A., Mara, P., Sehein, T., Wegener, G., Chambers, C.R., Joye, S.B., Peterson, R. N., Philippe, A., Burgaud, G., Edgcomb, V.P., Teske, A.P., 2021. Environmental factors shaping bacterial, archaeal and fungal community structure in hydrothermal sediments of Guaymas Basin, Gulf of California. PLOS ONE 16, e0256321.

Rao, C.R., 1982. Diversity and dissimilarity coefficients: a unified approach. Theor. Popul Biol. 21, 24–43.

Riedel, T., Biester, H., Dittmar, T., 2012. Molecular fractionation of dissolved organic matter with metal salts. Environ. Sci. Technol. 46, 4419–4426.

Robinson, K.J., Gould, I.R., Fecteau, K.M., Hartnett, H.E., Williams, L.B., Shock, E.L., 2019. Deamination reaction mechanisms of protonated amines under hydrothermal conditions. Geochim. Cosmochim. Acta 244, 113–128.

Rossel, P.E., Stubbins, A., Rebling, T., Koschinsky, A., Hawkes, J.A., Dittmar, T., 2017. Thermally altered marine dissolved organic matter in hydrothermal fluids. Org. Geochem. 110, 73–86.

Sarkar, S., Moser, M., Berndt, C., Doll, M., Böttner, C., Chi, W.-C., Klaeschen, D., Galerne, C., Karstens, J., Geilert, S., Mortera-Gutierrez, C., Hensen, C., 2022. Thermal state of the Guaymas Basin derived from gas hydrate bottom simulating reflections and heat flow measurements. J. Geophys. Res. Solid Earth 127, e2021JB023909.

Schmidt, F., Elvert, M., Koch, B.P., Witt, M., Hinrichs, K.-U., 2009. Molecular characterization of dissolved organic matter in pore water of continental shelf sediments. Geochim. Cosmochim. Acta 73, 3337–3358.

Schmidt, F., Koch, B.P., Witt, M., Hinrichs, K.-U., 2014. Extending the analytical window for water-soluble organic matter in sediments by aqueous Soxhlet extraction. Geochim. Cosmochim. Acta 141, 83–96.

Seidel, M., Beck, M., Riedel, T., Waska, H., Suryaputra, I.G.N.A., Schnetger, B., Niggemann, J., Simon, M., Dittmar, T., 2014. Biogeochemistry of dissolved organic matter in an anoxic intertidal creek bank. Geochim. Cosmochim. Acta 140, 418–434.

Seidel, M., Manecki, M., Herlemann, D.P., Deutsch, B., Schulz-Bull, D., Jürgens, K., Dittmar, T., 2017. Composition and transformation of dissolved organic matter in the Baltic Sea. Front. Earth Sci. 5, 31.

Seidel, M., Yager, P.L., Ward, N.D., Carpenter, E.J., Gomes, H.R., Krusche, A.V., Richey, J.E., Dittmar, T., Medeiros, P.M., 2015. Molecular-level changes of dissolved organic matter along the Amazon River-to-ocean continuum. Mar. Chem. 177, 218–231.

Simoneit, B.R., Kvenvolden, K.A., 1994. Comparison of 14C ages of hydrothermal petroleums. Org. Geochem. 21, 525–529.

Simoneit, B.R., Lonsdale, P.F., 1982. Hydrothermal petroleum in mineralized mounds at the seabed of Guaymas Basin. Nature 295, 198–202.

Simoneit, B.R.T., 2018. Hydrothermal petroleum. In: Wilkes, H. (Ed.), Hydrocarbons, Oils and Lipids: Diversity, Origin, Chemistry and Fate. Springer International Publishing, Cham, pp. 1–35.

Simoneit, B.R.T., Schoell, M., 1995. Carbon isotope systematics of individual hydrocarbons in hydrothermal petroleums from the Guaymas Basin, Gulf of California. Org. Geochem. 23, 857–863.

Stenson, A.C., 2008. Reversed-phase chromatography fractionation tailored to mass spectral characterization of humic substances. Environ. Sci. Technol. 42, 2060–2065.

Teske, A., 2024. The Guaymas Basin – a hot spot for hydrothermal generation and anaerobic microbial degradation of hydrocarbons. Int. Biodeter. Biodegr. 186, 105700.

Teske, A., Callaghan, A.V., LaRowe, D.E., 2014. Biosphere frontiers of subsurface life in the sedimented hydrothermal system of Guaymas Basin. Front. Microbiol. 5, 99933.

Teske, A., Lizarralde, D., Höfig, T., Aiello, I., Ash, J., Bojanova, D., Buatier, M., Edgcomb, V., Galerne, C., Gontharet, S., Heuer, V., Jiang, S., Kars, M., Singh, K., Kim, J., Koorneef, L., Marsaglia, K., Meyer, N., Morono, Y., Negrete-Aranda, R., Neumann, F., Pastor, L., Peña-Salinas, M., Pérez-Cruz, L., Ran, L., Riboulleau, A., Sarao, J., Schubert, F., Stock, J., Toffin, L., Xie, W., Tamanaka, T., Zhuang, G., 2021a. Expedition 385 methods. In: Teske, A.P., Höfig, T.W., Expedition Scientists (Eds.), Guaymas Basin Tectonics and Biosphere. Proceedings of the International Ocean Discovery Program.

Teske, A., Lizarralde, D., Höfig, T., Aiello, I., Ash, J., Bojanova, D., Buatier, M., Edgcomb, V., Galerne, C., Gontharet, S., Heuer, V., Jiang, S., Kars, M., Singh, K., Kim, J., Koorneef, L., Marsaglia, K., Meyer, N., Morono, Y., Negrete-Aranda, R., Neumann, F., Pastor, L., Peña-Salinas, M., Pérez-Cruz, L., Ran, L., Riboulleau, A., Sarao, J., Schubert, F., Stock, J., Toffin, L., Xie, W., Tamanaka, T., Zhuang, G., 2021b. Expedition 385 summary. In: Teske, A.P., Höfig, T.W., Expedition Scientists (Eds.), Proceedings of the International Ocean Discovery Program.

Teske, A., Lizarralde, D., Höfig, T., Aiello, I., Ash, J., Bojanova, D., Buatier, M., Edgcomb, V., Galerne, C., Gontharet, S., Heuer, V., Jiang, S., Kars, M., Singh, K., Kim, J., Koorneef, L., Marsaglia, K., Meyer, N., Morono, Y., Negrete-Aranda, R., Neumann, F., Pastor, L., Peña-Salinas, M., Pérez-Cruz, L., Ran, L., Riboulleau, A., Sarao, J., Schubert, F., Stock, J., Toffin, L., Xie, W., Tamanaka, T., Zhuang, G., 2021c. Site U1545. In: Teske, A.P., Höfig, T.W., Expedition Scientists (Eds.), Guaymas Basin Tectonics and Biosphere. Proceedings of the International Ocean Discovery Program.

Teske, A., Lizarralde, D., Höfig, T., Aiello, I., Ash, J., Bojanova, D., Buatier, M., Edgcomb, V., Galerne, C., Gontharet, S., Heuer, V., Jiang, S., Kars, M., Singh, K., Kim, J., Koorneef, L., Marsaglia, K., Meyer, N., Morono, Y., Negrete-Aranda, R., Neumann, F., Pastor, L., Peña-Salinas, M., Pérez-Cruz, L., Ran, L., Riboulleau, A., Sarao, J., Schubert, F., Stock, J., Toffin, L., Xie, W., Tamanaka, T., Zhuang, G., 2021d. Site U1550. In: Teske, A.P., Höfig, T.W., Expedition Scientists (Eds.), Guaymas Basin Tectonics and Biosphere. Proceedings of the International Ocean Discovery Program.

Teske, A., Lizarralde, D., Höfig, T., Aiello, I., Ash, J., Bojanova, D., Buatier, M., Edgcomb, V., Galerne, C., Gontharet, S., Heuer, V., Jiang, S., Kars, M., Singh, K., Kim, J., Koorneef, L., Marsaglia, K., Meyer, N., Morono, Y., Negrete-Aranda, R., Neumann, F., Pastor, L., Peña-Salinas, M., Pérez-Cruz, L., Ran, L., Riboulleau, A., Sarao, J., Schubert, F., Stock, J., Toffin, L., Xie, W., Tamanaka, T., Zhuang, G., 2021e. Site U1551. In: Teske, A.P., Höfig, T.W., Expedition Scientists (Eds.), Guaymas Basin Tectonics and Biosphere. Proceedings of the International Ocean Discovery Program.

Teske, A., Lizarralde, D., Höfig, T., Aiello, I., Ash, J., Bojanova, D., Buatier, M., Edgcomb, V., Galerne, C., Gontharet, S., Heuer, V., Jiang, S., Kars, M., Singh, K., Kim, J., Koorneef, L., Marsaglia, K., Meyer, N., Morono, Y., Negrete-Aranda, R., Neumann, F., Pastor, L., Peña-Salinas, M., Pérez-Cruz, L., Ran, L., Riboulleau, A., Sarao, J., Schubert, F., Stock, J., Toffin, L., Xie, W., Tamanaka, T., Zhuang, G., 2021f. Sites U1547 and U1548. In: Teske, A.P., Höfig, T.W., Expedition Scientists (Eds.), Guaymas Basin Tectonics and Biosphere. Proceedings of the International Ocean Discovery Program.

Teske, A., McKay, L.J., Ravelo, A.C., Aiello, I., Mortera, C., Núñez-Useche, F., Canet, C., Chanton, J.P., Brunner, B., Hensen, C., Ramírez, G.A., Sibert, R.J., Turner, T., White, D., Chambers, C.R., Buckley, A., Joye, S.B., Soule, S.A., Lizarralde, D., 2019. Characteristics and evolution of sill-driven off-axis hydrothermalism in Guaymas Basin – the Ringvent site. Sci. Rep. 9, 13847.

Valle, J., Gonsior, M., Harir, M., Enrich-Prast, A., Schmitt-Kopplin, P., Bastviken, D., Conrad, R., Hertkorn, N., 2018. Extensive processing of sediment pore water dissolved organic matter during anoxic incubation as observed by high-field mass spectrometry (FTICR-MS). Water Res. 129, 252–263.

van Dongen B, E. , Schouten S, Sinninghe Damsté JS (2002) Carbon isotope variability in monosaccharides and lipids of aquatic algae and terrestrial plants. Marine Ecology Progress Series, 232: 83-92.

Vieth, A., Mangelsdorf, K., Sykes, R., Horsfield, B., 2008. Water extraction of coals–potential for estimating low molecular weight organic acids as carbon feedstock for the deep terrestrial biosphere. Org. Geochem. 39, 985–991.

Wagner, S., Jaffé, R., Stubbins, A., 2018. Dissolved black carbon in aquatic ecosystems. Limnol. Oceanogr. Lett. 3, 168–185.

Wang, L., Lin, Y., Ye, L., Qian, Y., Shi, Y., Xu, K., Ren, H., Geng, J., 2021. Microbial roles in dissolved organic matter transformation in full-scale wastewater treatment processes revealed by reactomics and comparative genomics. Environ. Sci. Technol. 55, 11294–11307.

Yamashita, Y., Mori, Y., Ogawa, H., 2023. Hydrothermal-derived black carbon as a source of recalcitrant dissolved organic carbon in the ocean. Sci. Adv. 9, eade3807.